

1 **Determinants for the Subcellular Localization and Function of a Non-essential**
2 **SEDS protein**

3

4 Gonçalo Real^{1,4}, Allison Fay^{2,4}, Avigdor Eldar³, Sérgio M. Pinto^{1,5}, Adriano O. Henriques¹,
5 Jonathan Dworkin^{*2}

6

7 ¹Instituto de Tecnologia Química e Biológica, Universidade Nova de Lisboa, Av. da
8 República, Apartado 127, 2781-901 Oeiras, PORTUGAL

9 ²Department of Microbiology, College of Physicians and Surgeons, Columbia University,
10 New York, NY 10032

11 ³Division of Biology, California Institute of Technology, Pasadena, CA 94703

12

13 ⁴These authors contributed equally to the work

14 ⁵Present address: Institute for Molecular Biology, University of Zurich, Zurich, Switzerland.

15

16 Running title: Analysis of Non-essential SEDS protein

17

18

19 ^{*}Corresponding author. Mailing address: Department of Microbiology, College of

20 Physicians and Surgeons, Columbia University, 701 W. 168th St., New York, NY 10032.

21 Phone: (212) 342-3731. Fax: (212) 305-1468. Email: jonathan.dworkin@columbia.edu

22

23

24

24 **Abstract**

25

26 The *B. subtilis* SpoVE integral membrane protein is essential for the heat resistance of
27 spores probably because of its involvement in spore peptidoglycan synthesis. We found
28 that a SpoVE-YFP fusion protein becomes localized to the forespore during the earliest
29 stages of engulfment, and this pattern is maintained throughout sporulation. SpoVE
30 belongs to a well-conserved family of proteins that includes the FtsW and RodA proteins
31 of *B. subtilis*. These proteins are involved in bacterial shape determination, although their
32 function is not known. FtsW is necessary for the formation of the asymmetric septum in
33 sporulation, and we found that an FtsW-YFP fusion localized to this structure, prior to the
34 initiation of engulfment in a non-overlapping pattern with SpoVE-CFP. Since FtsW and
35 RodA are essential for normal growth, it has not been possible to identify loss-of-function
36 mutations that would greatly facilitate analysis of their function. We took advantage of the
37 fact that SpoVE is not required for growth to obtain point mutations in SpoVE that block
38 the development of spore heat resistance, but that allow normal protein expression and
39 targeting to the forespore. These mutant proteins will be invaluable tools for future
40 experiments aimed at elucidating the function of members of the SEDS family of proteins.

41 Introduction

42

43 Bacterial shape is determined by an extracellular structure composed of peptidoglycan
44 (PG), a rigid polymer of repeated subunits of a disaccharide peptide monomer. This giant
45 macromolecule is found on the outside of the cytoplasmic membrane of nearly all
46 eubacteria. A series of essential and highly conserved enzymes convert UDP-GlcNAc to
47 Lipid II, the UDP-muramyl pentapeptide (51). To form mature PG, Lipid II is translocated
48 across the cytoplasmic membrane via an uncharacterized mechanism and is added to the
49 pre-existing cell wall through transpeptidation and transglycosylation reactions mediated by
50 members of the PBP (Penicillin Binding Protein) family of proteins. Little is known about the
51 mechanism of Lipid II transport across the cytoplasmic membrane other than it is probably
52 dependent on a protein(s) since it does not occur spontaneously across lipid bilayers (50).

53 The integral membrane proteins RodA and FtsW are members of what has been
54 termed the SEDS (“shape, elongation, division and sporulation”) family of integral
55 membrane proteins (18, 20) present in all cell wall-containing bacteria. Several lines of
56 evidence are consistent with the participation of RodA and FtsW in the translocation of
57 Lipid II during cell elongation and cell division, respectively (19, 21) although this
58 hypothesis has not been subjected to a direct test. For instance, depletion of RodA leads
59 to a block in lateral cell growth (18), although RodA is not strictly essential for cell viability.
60 Null mutants exhibit slow growth and small cell diameters and are viable in minimal
61 medium (7). Also, temperature sensitive *E. coli ftsW* mutations lead to blocks at both early
62 and late stages of cell division (26, 27), suggesting that FtsW acts during both initiation
63 and septum maturation (3).

64 RodA and FtsW are likely to function as part of essential elongation and division
65 complexes for PG synthesis (19). Each complex is thought to include one protein from
66 the SEDS family and one PBP (although several PBP proteins may associate with a
67 single SEDS protein) (21). Mutations in *E. coli ftsI* (encoding PBP3) that lead to a reduced
68 ability to divide can be suppressed by *rodA* mutations that, by themselves, interfere with
69 normal cell growth (1). FtsW from *Mycobacterium tuberculosis* interacts with penicillin-
70 binding protein 3 (6) and *E. coli* FtsW interacts with PBP2 in two different bacterial two
71 hybrid assays (23). The formation of PG on isolated *E. coli* membranes requires the
72 presence of high levels of both RodA and PBP2 proteins (21). These observations are
73 consistent with the proposed role of the SEDS proteins in Lipid II translocation. However,
74 the essential nature of FtsW and RodA makes testing this hypothesized function difficult.
75 Thus, either temperature sensitive (27) or depletion strains (3, 18) must be used to
76 evaluate the properties of FtsW or RodA. One issue complicating the interpretation of
77 experiments based on such strains is that a reduced rate of Lipid II translocation could be
78 due to the absence of the proteins or to a general loss in viability.

79 Fortunately, a third SEDS family member functions during the non-essential process of
80 sporulation in *B. subtilis* (20, 22). Bacterial endospores can survive extremes of heat and
81 desiccation, largely because of the presence of the spore cortex. This structure is
82 composed of a form of PG that is similar, although not identical, to vegetative PG with
83 fewer peptide side chains, a concomitant reduction in the crosslinking of the glycan
84 strands, and the presence of muramic δ -lactam residues (56-58). Sporulation in *B.*
85 *subtilis* begins with an asymmetric division creating a smaller forespore and a larger
86 mother cell. During the process of engulfment, the forespore compartment becomes

87 completely enclosed in the mother cell and it is surrounded by two membranes possibly
88 separated by a thin layer of PG. Assembly of the spore PG then occurs in the space
89 between the two membranes resulting from the action of genes expressed in the mother
90 cell compartment (40). *spoVE*, which during sporulation is expressed under the control of
91 the mother cell-specific transcription factor σ^E (49), is not essential for vegetative growth
92 yet it is absolutely required for the production of cortex PG. Thus, during sporulation,
93 $\Delta spoVE$ mutants fail to form a cortex (17, 38, {Vasudevan, 2007 #832}) and they
94 accumulate cytoplasmic PG precursors (54), suggesting a defect at an early step in PG
95 polymerization and consistent with the view that the SEDS proteins may function in lipid-
96 linked precursor translocation. SpoVE may be part of a third putative PG biosynthetic
97 complex of *B. subtilis* and other endospore-forming bacteria which includes a sporulation-
98 specific, σ^E -controlled PBP, called SpoVD, required for synthesis of the cortex (4). It is
99 interesting to note that both *spoVE* (which occupies the position of *ftsW*) and *spoVD* are
100 located in the *dcw* cluster of spore-forming bacteria, perhaps because coordinated
101 expression of *dcw* genes is important for synthesis of the spore cortex ({Real, 2006
102 #821}).

103 The large number of mother cell-expressed membrane proteins that localize to the
104 outer forespore membrane (52, 53) suggests that SpoVE might localize in a similar
105 fashion. Some mother cell-expressed membrane proteins can be found distributed in all
106 accessible membranes, particularly in the absence of appropriate “anchoring” proteins
107 (43). Since spore cortex synthesis occurs underneath the outer forespore membrane, it is
108 thus reasonable to expect that SpoVE would localize to this membrane.

109 Finally, since the spore cortex layer is essential to providing the heat resistance of
110 spores, the loss of heat resistance is a convenient assay for SpoVE function (32). Since
111 heat resistance can be accurately measured over several orders of magnitude, SpoVE
112 mutants can be quantitatively differentiated. Therefore, the ability to examine the
113 phenotype of loss-of-function *spoVE* mutants will greatly facilitate studies of the role of
114 SpoVE in cortex biogenesis and is also likely to provide insight into the function of the
115 SEDS family of proteins.

ACCEPTED

116 **Materials and Methods**

117

118 Standard procedures were used to prepare and handle recombinant DNA and to
119 transform *E. coli* cells. *B. subtilis* strains were derivatives of PY79 unless noted (59) and
120 *E. coli* strains used were DH5, TG1, or CC118(DE3)pLysS. *B. subtilis* was transformed
121 using competent cells made by the two-step method (16). Sporulation for microscopy
122 used either Difco sporulation medium (DSM) (16) or CH medium for growth and A+B
123 medium for resuspension (48). Heat resistance of spores was assayed following
124 sporulation by exhaustion in DSM medium in 2ml cultures for 24 hours. Serial dilutions
125 were plated before and after the cells were heated to 80°C or 55°C for 20 minutes. CFU's
126 were compared from before and after heat treatment.

127

128 **Strain construction**

129 Strains are listed in Table 1. For details of construction, see Supplementary Table 1.

130

131 **Plasmid construction**

132 Supplementary Table 2 lists plasmids and details of their construction. Oligonucleotides
133 used are listed in Supplementary Table 2

134

135 **Fluorescence Microscopy**

136 Samples of DSM cultures for visualization of fluorescence were prepared as previously
137 described (41). For visualization of DNA and membranes, 4,6-diamidino-2-phenylindole
138 dihydrochloride (DAPI; 1 mg/ml stock) and membrane dye FM4-64 (Molecular Probes,

139 100 mg/ml stock) were added to cells at a final concentration of 10 μ g/ml prior to mounting
140 on agarose-coated slides. All samples were observed with a 63x objective lens. Phase
141 contrast or fluorescence images were acquired with a Leica DMRA2 Microscope coupled
142 CoolSNAP™ HQ Photometrics camera (Roper Scientific, Tucson, Arizona), recorded and
143 processed for publication using Adobe Photoshop, version 6.0.

144 For cultures in resuspension medium, 100 μ l of sporulating cells were taken at designated
145 times after resuspension. To each sample, 0.5 μ l of FM4-64 (100 mg/ml) was added just
146 before the cells were collected by centrifugation. The pellet was resuspended in 10 μ l
147 PBS, and added to a poly-L-lysine pre-treated coverslip. All microscopy was performed on
148 a Nikon Eclipse 90i with a 100X objective using phase contrast and captured by a
149 Hamamatsu Orca-ER camera using Nikon Elements BR software. Exposure for FITC and
150 TRITC was 800ms for all pictures taken. For the SpoVE-CFP, FtsW-YFP time-course, the
151 strain (JDB1678) was sporulated by resuspension and at the designated times, samples
152 were taken and prepared as mentioned above. Line scans of fluorescence on images
153 were performed using Nikon BR Elements software.

154

155 **Time-lapse movies**

156 Strain JDB1835 was grown in CH medium to an OD of 0.6 and then resuspended in equal
157 volume of A+B resuspension medium (48) for 1.5h and then put on a 1.5% w/v low
158 melting point agarose (Sigma) pad made from fresh A+B and cut into a \sim 1cm² square.
159 Pads were sealed in a glass bottom dish (Wilco Wells, Netherland) with bacteria facing
160 down and were imaged with an epifluorescence inverted Olympus BX-61 microscope

161 every 7 min using a xenon lamp and a GFP filter-cube. Under these conditions, the
162 bacteria grew an average of three cell divisions and then sporulated.

163

164 **Generation of *spoVE* mutants I58N, C82R, S103N, E116G, C160R, G292R, G355D.**

165 Plasmid pTC30 (lab stock) was constructed by inserting a fragment containing *PspoVE*-
166 *His₆-spoVE* between the *HindIII* and *EcoRI* sites of the pMLK83 shuttle vector (25).

167 Plasmid pTC30 was used to transform the mutator strain *E. coli* XL1-Red (Stratagene),
168 and transformants were selected on LB plates containing ampicillin (100 µg/ml).

169 Transformants were then pooled and grown overnight at 37°C in LB broth containing

170 ampicillin (100 µg/ml). Randomly mutated plasmid DNA extracted from this culture was

171 then used to transform *B. subtilis* strain SL666 (37) with selection for neomycin

172 resistance. Mutations leading to a Spo⁻ phenotype were identified following plating of

173 transformants on DSM medium. Sporulation deficient transformants were then streaked

174 onto TBAB plates containing 1% starch to confirm that the plasmid had integrated at the

175 *amyE* locus. From a total of 34 mutants obtained, only 7 showed missense mutations

176 within the *spoVE* coding sequence and one in the RBS. The remaining mutations were

177 insertions and deletions and were discarded.

178

179 **Generation of *spoVE* mutants: E271A, N322A, G335A, S341A, G343A, W69A, K76A,**

180 **T173A.**

181 We introduced alanine substitutions at specific positions in the SpoVE coding sequence

182 using the Quick Change site-directed mutagenesis kit (Stratagene). We used pCB41

183 plasmid carrying *amyE* flanking sequences and *P_{spoVE}-spoVE-gfp* as template and oligos

184 oJD104 (G335A), oJD106 (S341A), ojd108 (G343A), ojd142 (N322A) to generate
185 plasmids carrying these mutations: pAF150 = *spoVEE271A*, pAF155 = *spoVEN322A*,
186 pAF147 = *spoVEG335A*, pAF148 = *spoVES341A*, pAF149 = *spoVEG343A*. We used
187 pAF032 as template and oligonucleotides oAF302, oAF304, and oAF306, respectively to
188 generate plasmids carrying these mutations: pAFM302 = *spoVEW69A*, pAFM304 =
189 *spoVEK76A*, pAFM308 = *spoVET173A*.

190

191 **Construction of *spoVE'*-*phoA* fusions and assay for alkaline phosphatase activity.**

192 The *phoA* gene was excised from pPHO7 (15) with *XhoI* and *BamHI* and inserted
193 between the *Sall* and *BamHI* sites of pLITMUS29 generating pAH310. *phoA* was then
194 released from pAH310 with *SpeI* and *StuI* and inserted between the *SpeI* and *HincII* sites
195 of pBuescriptIIISK(+) to yield pAH312. A series of ten 3' truncations of *spoVE* were then
196 constructed by PCR using chromosomal DNA from MB24 as the template, *spoVE-10D* as
197 the forward primer and various reverse primers, chosen so that PhoA is fused after each
198 of the transmembrane segments predicted with the TMpred, TopPred and TM HMM
199 programs. All PCR products were digested with *PstI* and either *BamHI*, *BglII*, or *BclI* and
200 introduced into *PstI*- and *BamHI*-cut pAH312. The resulting plasmids, which were
201 sequenced to ensure that no undesired mutation was introduced, were used to transform
202 *E. coli* CC118(DE3)pLysS with selection for ampicillin. PhoA activity was detected as blue
203 colonies on LB agar plates containing 5-bromo-4-chloro-3-indolyl-phosphate (XP),
204 ampicillin, and chloramphenicol at concentrations of 40 $\mu\text{g/ml}$, 100 $\mu\text{g/ml}$, and 30 $\mu\text{g/ml}$,
205 respectively. The activity of alkaline phosphatase was also assayed in liquid cultures by
206 measuring the rate of *p*-nitrophenyl phosphate hydrolysis. The cells were grown at 37 °C

207 in LB to an OD₆₀₀ of 0.4–0.6, at which time IPTG (to 0.5 mM) was added to the cultures.
208 Growth continued for 2.5 h after which the cells were harvested and assayed for activity
209 (33).

210

211 **Construction of *spoVE*'-lacZ fusions and assay for β -galactosidase activity.**

212 Fusions of the SpoVE amino-terminal region to LacZ were constructed by amplification of
213 the *spoVE* fragments present in the pAH312 derivatives described above using primers
214 *spoVE*1D and *spoVE*-lacZR. The resulting fragments were digested with *EcoRI* and
215 *BamHI* and inserted between the *EcoRI* and *BamHI* sites of pNM480 {Minton, 1984
216 #881}. The resulting plasmids were used to transform *E. coli* CC118(DE3)pLysS with
217 selection for ampicillin. β -galactosidase activity was detected as blue colonies on LB agar
218 plates containing Xgal (5-bromo-4-chloro-3-indolyl- β -D-galactopyranoside), ampicillin, and
219 chloramphenicol at concentrations of 80 μ g/ml, 100 μ g/ml, and 30 μ g/ml, respectively. β -
220 galactosidase activity was assayed on liquid cultures by measuring the rate of hydrolysis
221 of o-nitrophenyl- β -galactopyranoside as described previously (35).

222

223 **Immunoblot analysis**

224 For DSM cultures, samples (10 ml) were collected and lysed as described before (45).
225 Samples (30 μ g) of total protein were resolved on 12% SDS-PAGE, and subjected to
226 immunoblot analysis (45). Anti-GFP antibody (laboratory stock) was used at a dilution of
227 1:1000. A rabbit secondary antibody conjugated to horseradish peroxidase (Sigma) was
228 used at dilutions of 1:10000. The immunoblots were developed with ECL plus (GE
229 Health).

230 For cultures in resuspension medium, at each time point OD_{600} was taken. Volumes of
231 samples were normalized to yield an OD_{600} of 0.50. After pelleting, cells were
232 resuspended and protoplasted in 100 μ l SMM with 1mg/ml lysozyme for 5 min at room
233 temperature. Protoplasts were then lysed after collection by resuspension in 100 μ l of 1x
234 sample buffer and solubilized for 30 min at 37°C. 20 μ l of each sample was loaded on a
235 13% polyacrylamide gel for SDS-PAGE. Gels were transferred to Biotrace-NT (Pall Life
236 Sciences) and probed using anti-GFP rabbit serum (generous gift of Howard Shuman,
237 1:25000), anti-rabbit-HRP (1:25000, Pierce), then ECL plus (GE Health).

238 Results

239 Localization of SpoVE

240 Like all other genes known to be required for spore cortex formation (54), *spoVE* is
241 under control of σ^E , a mother-cell specific transcription factor (49). Therefore, SpoVE is
242 likely to be found at the outer forespore membrane, surrounding the developing spore,
243 and facing the mother cell cytoplasm. We examined this possibility by constructing a C-
244 terminal fusion of SpoVE with YFP and observing its pattern of localization in sporulating
245 cells. This fusion, expressed from the *spoVE* promoter (P_{spoVE} -*spoVE-yfp*) and designed
246 for recombination at the ectopic *amyE* chromosomal locus, was fully functional because
247 when introduced into a strain carrying a *spoVE85* mutation {Piggot, 1986 #798}, it
248 restored wild type levels of spore heat resistance. Consistent with its dependence on σ^E ,
249 SpoVE-YFP is not observed in cells upon entry to sporulation (Fig. 1A, panels b, c). Two
250 hours after the onset of the process (or T2), however, some cells have entered
251 sporulation, as indicated by the formation of asymmetric septa (Fig. 1A, panel e) and at
252 T3, most cells contain either polar septa or engulfing forespores (Fig. 1A, panel h).
253 SpoVE-YFP fluorescence was first detected at T2 closely associated with septa or
254 engulfing forespores (Fig. 1A, panel f). Strikingly, at T2 or T3, YFP fluorescence was
255 rarely found associated with straight septa, but rather was typically found associated with
256 curved septa (Fig. 1A, panels f and i). Finally, at T6, nearly all of the cells appear to have
257 completed the engulfment process (Fig. 1A, panel k) and, again, a YFP signal can be
258 observed around those forespores (Fig. 1A, panel l). Thus, SpoVE localizes in a pattern
259 that closely matches the membrane dynamics of the engulfing forespores. Further, the
260 pattern at later time points (post T3) is consistent with the role of SpoVE in spore cortex

261 synthesis, a late (post-engulfment) event in sporulation (54). Examination of SpoVE-YFP
262 expression by immunoblotting analysis of samples taken at equivalent time points
263 demonstrated that the protein appeared at T3, consistent with the microscopy (data not
264 shown).

265 Since these experiments were performed under time-course conditions, it was not
266 possible to follow SpoVE localization in a single cell. We therefore employed time-lapse
267 microscopy to visualize the distribution of a functional SpoVE-GFP fusion every 7 min in a
268 single cell as it proceeded through sporulation (Fig 1B). Initially, SpoVE-GFP was
269 observed as a single, slightly curved band (Fig. 1B, panel a), consistent with our time
270 course observations (Fig. 1A, panel f). As the cell continued to undergo sporulation, the
271 SpoVE-GFP signal followed the expected pattern of a protein associated with an
272 engulfing forespore (Fig. 1B, panels b, c, d) and at the final time point (Fig. 1B, panel e),
273 the signal surrounded the (presumably) engulfed forespore. This experiment confirms the
274 time-course data in that SpoVE appears absent from polar septa prior to the initiation of
275 engulfment (when the septa become curved), and that its distribution thereafter closely
276 mimics the engulfing outer forespore membrane.

277

278 **Localization of SpoVE and FtsW in vegetative cells**

279 The apparent absence of SpoVE from straight polar septa was intriguing, because
280 another SEDS protein, *E. coli* FtsW, associates with division septa (3, 26), and because
281 SpoVE and its paralog *B. subtilis* FtsW (also expected to localize at division sites) are
282 highly similar along their entire primary structure. This prompted us to examine both the
283 localization of *B. subtilis* FtsW and whether production of SpoVE under vegetative

284 conditions would result in its localization to division sites at mid cell. We first examined the
285 localization of a functional FtsW-GFP fusion integrated at the *ftsW* locus of *B. subtilis*
286 during growth and sporulation. We observed this strain during vegetative growth and
287 found that FtsW-GFP localized, as expected, to mid cell (Fig. 2A, panels a, b). In contrast,
288 no GFP signal was observed at a time during sporulation (T3, Fig 2A, panels c, d) when
289 most cells exhibit a SpoVE-GFP signal at the forespore.

290 The absence of an FtsW-GFP signal in sporulating cells did not reflect an absence of
291 FtsW-GFP protein because immunoblotting using anti-GFP antibodies revealed that
292 FtsW-GFP expression under control of P_{ftsW} was relatively constant during sporulation
293 (Fig. 2B). When FtsW-GFP was placed under control of the heterologous promoter P_{spoVE} ,
294 no fluorescent signal was seen during vegetative growth (Fig. 2A, panels e, f) consistent
295 with the sporulation-specific activity of the promoter. However, during sporulation, a GFP
296 signal was observed throughout all mother-cell membranes (Fig. 2A, panels g, h) in
297 contrast with the enrichment of SpoVE that we observed at the outer forespore membrane
298 (Fig. 2A, panels o, p). The FtsW-GFP signal and the comparatively high level of FtsW-
299 GFP protein revealed by immunoblotting (Fig. 2C; compare with Fig. 2B) indicate that the
300 protein was present in sporulating cells but was not targeted to the forespore.

301 When we placed SpoVE-GFP under control of P_{ftsW} , the protein lacked discrete septal
302 localization; instead we observed a relatively faint signal in all cell membranes (data not
303 shown). To confirm that this pattern was not the result of a non-functional fusion protein,
304 we inserted P_{spoVE} upstream of P_{ftsW} such that SpoVE-GFP was under the control of both
305 promoters. During vegetative growth, this construct again resulted in no septal localization
306 (Fig. 2A, panels i, j), although a membrane associated fluorescent signal was observed

307 that was absent in cells expressing SpoVE-GFP under the control of its endogenous
308 P_{spoVE} promoter (Fig. 2A, panels m, n). When the $P_{spoVE^-}P_{ftsW^-}spoVE-gfp$ strain was
309 sporulated, a GFP signal was observed at the forespore (Fig. 2A, panels k, l), similar to
310 that seen with $P_{spoVE^-}spoVE-GFP$ strain (Fig. 2A, panels o, p), indicating that the SpoVE
311 construct was functional. Thus, SpoVE-GFP appears to be excluded from both vegetative
312 and polar septa, while FtsW-GFP fails to localize to the engulfing membranes during
313 sporulation. These differences in the subcellular distribution of SpoVE-GFP and FtsW-
314 GFP likely reflect the activity of different targeting signals contained in their primary
315 sequence.

316

317 **FtsW and SpoVE have non-overlapping patterns of localization.**

318 The likely involvement of FtsW in polar division suggests that the protein localizes to
319 sites of asymmetric division. However, this localization must be transient since FtsW-GFP
320 localization to the forespore membranes was not detected by hour 3 of sporulation when
321 asymmetric division is complete in most cells and the process of engulfment commences
322 (see above). This suggests that FtsW is no longer detected in those cells initiating the
323 engulfment process and in which the localization of SpoVE is first detected. To investigate
324 this possibility, we examined the cellular distribution of FtsW and SpoVE simultaneously
325 in sporulating cells. We constructed a strain expressing both a complementing FtsW-YFP
326 fusion under control of P_{ftsW} and a complementing SpoVE-CFP fusion under of P_{spoVE^-} . We
327 quantified the fluorescence in >20 cells at each time point by measuring the pixel intensity
328 for both the CFP and YFP channels along a line drawn length-wise along the cell. The
329 traces chosen represent a typical cell. At 30 min following resuspension, some cells

330 contained a discrete focus of YFP signal at mid-cell, consistent with the completion of the
331 last round of division, but lacked a CFP signal, consistent with the expected lack of σ^E
332 expression at this time (Fig. 3). At 75 minutes, cells began to contain asymmetric septa
333 associated with an YFP signal, but still no CFP signal. Starting at 90 minutes following
334 resuspension, some of these septa started to curve, and were now associated with a CFP
335 signal, but little YFP signal. This difference between the CFP and YFP signals became
336 even more pronounced at later time points (Fig. 3; T=105 min, T150 min). Thus, FtsW
337 and SpoVE have non-overlapping patterns of localization at the sporulation septum, with
338 FtsW-YFP present at the time of asymmetric septation, but disappearing at or before the
339 time of the initiation of engulfment followed by the observation of SpoVE-CFP only at
340 curving asymmetric septa. This morphological event is coupled to the activation of σ^E (39),
341 consistent with the known dependence of *spoVE* expression on σ^E .

342 The loss of FtsW-GFP signal upon the initiation of membrane curvature could result
343 from protein degradation, or alternatively, on the dilution of the GFP signal as the protein
344 becomes delocalized from the septal membrane and enters the much larger mother cell
345 membrane. FtsW-GFP levels as determined by immunoblotting cell lysates from
346 sporulating strains carrying FtsW-GFP alone were not different at times early in
347 sporulation as compared with later times (Figure 2B). We confirmed that the absence of a
348 GFP signal did not reflect a substantial decrease in overall cellular FtsW levels because
349 immunoblotting using anti-GFP antibodies revealed that FtsW-GFP expression under
350 control of P_{ftsW} was relatively constant (albeit lower) during sporulation as compared with
351 expression of FtsW under P_{spoVE} control (Fig. 2B, C). Thus, FtsW is likely to become
352 delocalized rather than degraded.

353

354 **Generation of SpoVE point mutants**

355 Unlike FtsW and RodA, SpoVE is not essential for normal growth; a strain carrying a
356 *spoVE* mutation appears completely normal for vegetative growth but results in the
357 production of heat sensitive spores. We took advantage of this characteristic to identify
358 mutations in *spoVE* that block function using two strategies. First, we randomly
359 mutagenized plasmids containing a *spoVE* gene by passage through an *E. coli* mutator
360 strain. Pooled plasmids from the mutagenesis were then transformed into a strain that
361 carried a *spoVE::kan* insertion mutation. The plasmid contained *amyE* sequences flanking
362 the *spoVE* gene, favoring integration to (and usually disrupting) the *amyE* locus. Amylase⁻
363 transformants were screened for Spo⁻ phenotype on DSM medium, and in this manner we
364 identified 6 *spoVE* missense mutations, *spoVEI58N*, *spoVEC82R*, *spoVES103N*,
365 *spoVEI116G*, *spoVEC160R*, *spoVEG292R* and *spoVEG355D* (Fig. 4A; see
366 Supplementary Fig. 1 for conservation of these positions among SEDS orthologs). Note
367 that *spoVEG355D* is the same mutation found in strain SL666 (Table 1), bearing the
368 *spoVE85* classical allele {Piggot, 1986 #798}.

369 As a second, complementary, strategy of *spoVE* mutagenesis, we used Pfam (10) to
370 generate a Hidden Markov model (44) of SEDS proteins from diverse bacterial species
371 (~500) that identified well conserved residues (Fig. 4B). We then introduced alanine
372 substitutions into several of these positions in *B. subtilis* SpoVE by site-directed
373 mutagenesis of a plasmid carrying a SpoVE-GFP fusion that was subsequently integrated
374 into the chromosome at the ectopic *amyE* locus (*spoVEE271A*, *spoVEG335A*,
375 *spoVES341A*, *spoVEG343A*; Fig. 4A). We also generated a second HMM, this time using

376 only SpoVE proteins, and again identified residues (Fig. 4B) that are conserved in SpoVE
377 proteins from diverse spore-formers, but not in other SEDS proteins. We then introduced
378 alanine substitutions in several of these positions in a *B. subtilis* SpoVE-GFP plasmid-
379 borne fusion that was subsequently integrated at *amyE* (*spoVEW69A*, *spoVEK76A*,
380 *spoVET173A*; Fig. 4A).

381

382 **Characterization of SpoVE point mutations: heat resistance**

383 SpoVE is absolutely required for the development of heat resistance since no colony
384 forming units are obtained following exposure of $\Delta spoVE::tet$ spores to 80°C for 20 min
385 (data not shown). We took advantage of this requirement to assess the functionality of
386 each of the *spoVE* point mutants we generated and determined the heat resistance of
387 spores carrying a mutant *spoVE* allele in the absence of the wild-type copy. All mutations
388 (I58N, C82R, S103N, E116G, C160R, G292R, and G355D) generated by random
389 mutagenesis resulted in a complete loss of spore heat resistance (Table 2). Similarly,
390 most of the spores carrying alanine substitutions introduced by site directed mutagenesis
391 in the C-terminus of SpoVE (E271A, G335A, S341A, G343A) were no longer heat
392 resistant (Table 2). The only exception to this pattern were spores with the N322A
393 mutation that were somewhat heat resistant, and this resistance was dependent on
394 temperature, as a less stringent heat treatment (55°C, 20 min) increased spore survival to
395 about 10% as compared to 0.19% at 80°C (data not shown). In contrast to the phenotype
396 of most of the C-terminal mutations, spores carrying mutations in the N-terminal end of
397 SpoVE (W69A, K76A, T173A) were somewhat heat resistant, albeit at <1% of the wild-
398 type (Table 2) and none of these mutants exhibited a temperature dependence of

399 survival. The inability of each of these SpoVE mutants to complement fully the loss of
400 heat resistance of a *spoVE::tet* mutation demonstrates that both mutagenesis strategies
401 successfully identified *spoVE* mutations that led to a loss of function. However, the heat-
402 kill data do not permit discrimination between potential causes of this loss of function
403 including increased protein degradation or aberrant protein localization. To address these
404 possibilities, we examined the localization and expression of each of these mutant SpoVE
405 proteins.

406

407 **Characterization of SpoVE point mutations: protein localization**

408 We took advantage of the ability of the SpoVE-YFP and SpoVE-GFP fusion proteins
409 to fully complement either *spoVE85* or $\Delta spoVE::tet$ mutations, respectively, to observe the
410 cellular distribution of the SpoVE point mutants. Since the fluorescent signal derived from
411 a SpoVE-YFP fusion is enriched at the outer forespore membrane (Fig. 1), we examined
412 cells expressing mutant SpoVE-GFP fusion proteins at T2.5 of sporulation using a
413 resuspension protocol. The fluorescent signal of SpoVE-GFP mutants containing alanine
414 substitutions in C-terminal residues (G335A, S341A, G343A, N322A, E271A) was
415 enriched at the forespore membrane, similar to wild-type SpoVE-GFP (Fig. 5A). By
416 contrast, SpoVE-GFP mutants with alanine substitutions (W69A, K76A, T173A) in their N-
417 terminal domain were no longer concentrated at the forespore (Fig. 5A). In the case of the
418 SpoVE-YFP mutant proteins, those carrying the S103N and E116G mutations were still
419 enriched at the forespore but other mutant proteins appeared to be expressed at lower
420 levels (I58N, G292R, G355D) or not at all (C82R, C160N) and were not appreciably
421 enriched at the forespore (Fig. 5B).

422 Since the double membrane of the forespore can obscure qualitative impressions of
423 forespore localization, we measured the ratio of the mean GFP fluorescence along a line
424 across the middle of forespore to the mean GFP fluorescence along a line across the
425 middle of the mother cell (Fig. 5C). The first line crosses four mother-cell accessible
426 membranes and the second line crosses two mother cell accessible membranes. Thus, if
427 there is an equal distribution across all mother cell accessible membranes, then the ratio
428 = 2. Alternatively, a ratio > 2 indicates that the fluorescent signal is enhanced at the
429 forespore and therefore that the protein preferentially localizes to the outer forespore
430 membrane. For wild-type SpoVE-GFP, the ratio was 3.51 +/-0.20. For the SpoVE
431 mutants that appeared to be enriched at the forespore, the ratios were: G335A = 3.34 +/-
432 0.21, S341A = 3.32 +/-0.33, G343A = 3.28 +/-0.19, N322A = 3.20 +/-0.12, E271A = 3.21
433 +/-0.22. For the SpoVE mutants that appeared evenly distributed, the ratios were: W69A
434 = 1.97 +/-0.15, K76A = 1.94 +/-0.13, T173A = 1.89 +/- 0.28). Thus, quantification of the
435 fluorescent signals yielded results consistent with the qualitative observations (Table 2).

436 Although inspection of the fluorescence microscopy images indicated that most
437 SpoVE-GFP mutant proteins and some SpoVE-YFP mutant proteins were expressed at
438 wild-type levels, a number of the SpoVE-YFP mutant proteins did not appear to be
439 expressed at all or were expressed at lower levels (Fig 5A, B). Since proper interpretation
440 of the loss-of-function phenotype observed in our measurements of spore heat resistance
441 (Table 2) depends on knowledge of protein expression levels, we examined lysates from
442 sporulating cells expressing different SpoVE-GFP mutants by Western analysis using an
443 anti-GFP antibody. The SpoVE-YFP mutants C82R and C160R were not detected in
444 lysates, similar to a strain lacking a SpoVE-YFP fusion (Fig. 6A). The fluorescent signal

445 for one of the SpoVE mutants, I58N was only slightly lower than that of the wild-type
446 SpoVE-YFP (wt); however two SpoVE mutants with similarly weak signals, G292R and
447 G355D, had both a reduced level of full-length protein and an increased level of free GFP
448 as compared to the wild-type strain. SpoVE mutants S103N and E126N that had wild type
449 fluorescent signal were expressed at levels similar, if not higher, than wild type. Thus, the
450 expression levels were consistent with the observed fluorescent signal, suggesting that
451 the loss of heat resistance of spores carrying most *spoVE-yfp* alleles was a result of
452 reduced accumulation of the various mutant forms of SpoVE-YFP.

453 When we examined the expression of the SpoVE-GFP mutant proteins, all of which
454 resulted in a substantial fluorescent signal (Fig. 5A), we observed full-length protein in all
455 cases following immunoblotting with anti-GFP antibodies, although the levels were greatly
456 reduced for the W69A, K76A, and T173A mutants as compared to the wild-type SpoVE-
457 GFP (wt). We observed additional bands at ~33 kDa that presumably is free GFP and at
458 ~ 38 kDa that we assume is a degradation product of SpoVE-GFP. The reduced heat
459 resistance of spores carrying W69A, K76A, and T173A mutations (Table 2) could
460 therefore be attributed to the lower protein levels, although the inability of the proteins to
461 be correctly targeted to the forespore (Fig. 5A) could also be a factor in this phenotype.
462 By contrast, the fact that spores carrying SpoVE G335A, G335A, S341A, G343A, and
463 N322A mutations were completely sensitive to heat (Table 2) cannot be explained by
464 defects in protein expression. Thus, these mutations must block the correct activity of
465 SpoVE, either by interfering with necessary protein-protein interactions or by preventing
466 the correct activity of the protein.

467

468 **Analysis of the membrane topology of SpoVE**

469 Although the high sequence conservation along the entire lengths of SpoVE and FtsW
470 suggests that they perform a similar function, they act at distinct times of the cycle (Figs.
471 2 and 3) and therefore likely interact with different protein(s). Consistent with this
472 expectation, FtsW interacts with components of the cell division apparatus (e.g. FtsZ (5))
473 that are not present at later stages (i.e. post-asymmetric division) where SpoVE acts (31).
474 The precise membrane topology of a SEDS protein may reflect these interactions and we
475 wanted to locate the functionally important residues identified in our mutagenesis of
476 *spoVE*. However, because the topological models available have been determined for
477 FtsW orthologs (5), we derived a topological model for SpoVE by constructing a series of
478 fusions of *spoVE* to *phoA* and to *lacZ*. Since alkaline phosphatase (AP) is only active
479 when present on the outside of the cell and, conversely, β -galactosidase is only active in
480 the cytoplasm, these two kinds of fusions provide a complementary readout of membrane
481 protein topology (33). The alkaline phosphatase or β -galactosidase activity of *E. coli* cells
482 harboring *spoVE'*-*phoA* and *-lacZ* plasmids was determined by blue and white screening
483 on plates containing the chromogenic substrates XP or X-Gal, respectively or in cells
484 grown in liquid medium and harvested during the exponential growth phase (see materials
485 and methods). The end points of the various PhoA or LacZ fusions and the corresponding
486 activities are indicated in Table 3. Fusions D40, G106, P162, S205, F228 and T262
487 showed high AP activity (> 88.5 Relative Units; note that background levels of AP activity
488 were of 14.8 RUs) suggesting the periplasmic localization of the PhoA moiety, whereas
489 fusions K76, P146, P300 and Y366 showed reduced AP activity (< 62.9 RUs; Table 3),
490 revealing the cytoplasmic localization of PhoA. Conversely, β -galactosidase activity was

491 only detected with fusions K76, P146, P300 and Y366 (Table 3) indicating the
492 cytoplasmic localization of the LacZ moiety (> 228.5 RUs; background levels of β -
493 galactosidase activity were 8.5 RUs). The accumulation of all fusion proteins was
494 confirmed by immunoblot analysis using antibodies against LacZ, PhoA and GFP (data
495 not shown). Together with the fluorescence of strains expressing either N- or C-terminal
496 fusion of SpoVE to GFP, which also serves as a reporter for cytoplasmic localization (9),
497 the results suggest a topology with both the N- and C-termini of SpoVE facing the
498 cytoplasm and separated by 10 transmembrane segments, with an extracellular loop of
499 71 residues located between TM 7 and TM 8 (Fig. 4A). The model is in agreement with
500 that proposed for the FtsW proteins of *E. coli* (28), *S. pneumoniae* (11), and
501 *Mycobacterium tuberculosis* (5), suggesting structural conservation at least among the
502 sporulation and cell division members of the SEDS family. The position of the various
503 point mutations characterized in this study is shown in figure 4A. Most of the mutations
504 map to predicted TM domains, but a few are in hydrophilic loops located in the cytoplasm
505 (K76A) or in the extracellular space between the mother cell and the forespore (S103R,
506 E271A, or G335A) (Fig. 4A). All of these affect highly conserved or invariant residues
507 among SEDS proteins. However, three mutations (W69A, C82R, and T173A) affect
508 residues absolutely conserved only among SpoVE orthologs (Fig. 4B).

509

510 Discussion

511 Many bacterial proteins display distinct patterns of subcellular distribution and where
512 the function of a protein is known, its pattern is often functionally relevant (46). Here we
513 have examined the sporulation-specific SpoVE integral membrane protein of *B. subtilis*.

514 Consistent with its essential role in spore heat resistance (38) and its involvement in
515 spore cortex synthesis (54), we find that SpoVE, as assayed by a fully complementing
516 SpoVE-YFP fluorescent protein fusion, is enriched at the forespore (Fig. 1). Since *spoVE*
517 is under control of the mother-cell specific transcription factor, σ^E , it is likely that this
518 enrichment is restricted to the outer forespore membrane and not to the inner forespore
519 membrane as well.

520 SpoVE localizes to the asymmetric septum very early in the process of membrane
521 engulfment (Fig. 1), as is seen with several other proteins. This early localization is
522 consistent with targeting of SpoVE to this septum early in its synthesis. However, our
523 experiments do not rule out that SpoVE is initially inserted into all accessible membranes
524 where it undergoes free diffusion before becoming “captured” by an anchoring protein in
525 the septum like SpoIIQ (2,8). While we do not know if this mechanism is responsible for
526 SpoVE forespore targeting, this possibility is certainly appealing.

527 Regardless of the mechanism that targets SpoVE to the forespore, our experiments
528 demonstrate that this mechanism is specific to SpoVE and not to other members of the
529 SEDS family. First, the forced production of FtsW during sporulation does not lead to a
530 similar pattern of localization as SpoVE (Fig. 2A). Second, FtsW and SpoVE have non-
531 overlapping patterns of localization at the asymmetric septum (Fig. 3) and this difference
532 occurs despite the presence of FtsW protein expressed from its own promoter (Fig. 2A).
533 Thus, the observed differences in the subcellular distribution of SpoVE and FtsW likely
534 reflect the activity of the different targeting signals intrinsic to their primary sequence. The
535 fact that FtsW seems to disappear from the spore membranes as sporulation proceeds
536 suggests that the role of the protein during this process is restricted to septation. In any

537 event, the similarity between FtsW and SpoVE along their entire primary sequence should
538 facilitate the identification of domains and/or residues responsible for these differences.

539 Here, we have taken advantage of the involvement of SpoVE in the non-essential
540 process of spore formation to identify point mutants in a SEDS protein that appear to be
541 true loss-of-function mutations. Although several *spoVE* alleles have been isolated before
542 {Piggot, 1986 #798; Piggot, 1976 #107}, they were not characterized, and with the
543 exception of *spoVE85* that we sequenced and found to be identical to the G355D
544 mutation generated in *E. coli*, they were probably lost. Therefore, this is the first isolation
545 and characterization of loss-of-function mutations in a SEDS protein. We used both
546 random and directed mutagenesis methods to identify residues that are important for heat
547 resistance, an easily scored phenotype that is dependent on SpoVE. We characterized
548 the localization and expression of these mutant SpoVE proteins and succeeded in
549 determining which of our original mutations did not interfere with either proper expression
550 or localization. Some of the mutations we obtained (W69A, K76A, C82R and T173A) were
551 in residues that are highly conserved within each group of proteins, SpoVE-, FtsW- or
552 RodA-like (Fig. 4B). For instance, the W at position 69 of SpoVE is substituted by a K in
553 FtsW orthologs, and by an L in RodA proteins, and C82 of SpoVE tends to be an L in
554 FtsW proteins, and a G in RodA proteins (Fig. 4B). Conceivably, these residues could be
555 involved in protein-protein interactions that are specific to PG-synthesis complexes
556 operating during elongation, division or cortex synthesis. If so, these interactions could be
557 involved in proper protein localization, as the W69A and C82R mutant forms of SpoVE
558 show deficient localization (Fig. 5 and Table 2). In contrast, some of the mutations found
559 in TM X of SpoVE affect residues that are absolutely conserved among the entire SEDS

560 family. These residues, e.g., G335, S341, and G343, may affect a functional aspect, such
561 as a specific protein-protein interaction that is essential for the activity of all SEDS
562 proteins. Consistent with this view, mutations as G335A, S341A, and G343A that affect
563 invariant residues do not affect the accumulation or localization of SpoVE (Fig. 5 and
564 Table 3). Thus, we may have identified mutations that block the correct functioning of
565 SpoVE, either by interfering with necessary protein-protein interactions or by preventing
566 the correct enzymatic activity of the protein. Presently, and in the absence of a functional
567 assay, we are unable to differentiate between those possible loss-of-function
568 mechanisms.

569 Although the phylogenetically conserved SEDS family of essential proteins involved
570 in cell division and growth was first characterized nearly 20 years ago, their function
571 remains largely unclear. The phenotypes of *ftsW* mutants, in particular, led to the
572 hypothesis that FtsW could be the missing ‘flippase’ responsible for the translocation of
573 Lipid II across the cytoplasmic membrane (19). Although PG synthesis is a very well
574 characterized metabolic pathway, with crystal structures for most of the enzymes
575 determined (47) and the identification of small molecule inhibitors specific to many of the
576 enzymatic steps (12), the mechanism of Lipid II translocation and, in fact, the proteins that
577 mediate this process remain unknown. Despite the evident appeal of the model that
578 posits SEDS proteins in this role, and additional observations consistent with predicted
579 protein interactions [e.g., FtsW and PBP3 in mycobacteria (6)], no direct evidence for this
580 proposed role has emerged. One reason for the absence likely lies in the requirement for
581 FtsW (and to a lesser extent, RodA) for growth under normal conditions. Temperature
582 sensitive mutants (27) or depletion strains (3, 18) of FtsW or RodA could be useful in this

583 regard, although the likelihood that FtsW and RodA use the same substrate (34) would
584 complicate such analysis. Thus, the generation of a spectrum of point mutants and of a
585 null mutant of the SpoVE SEDS protein as described herein will facilitate the development
586 of strategies aimed at demonstrating its function using either *in vivo* (29) or *in vitro* (36)
587 approaches.

588

589 **Acknowledgments**

590 We thank Colin Manoil for the gift of strains, Teresa Costa for the construction of pTC30,
591 and Anabela Isidro for the anti-GFP antibody. This work was funded by grants
592 POCTI/BCI/48647/2002 and POCI/BIA-BCM/60855/2004 from the “Fundação para a
593 Ciência e a Tecnologia” (F.C.T.) to A.O.H. and by an Irma T. Hirschl Scholar award and
594 startup funds from the Department of Microbiology, Columbia University to J.D. G.R. was
595 the recipient of a post-doctoral fellowship (SFRH/BPD/20668/2004) from the F.C.T. A.J.F.
596 was supported by NIH training grant AI007161-29.

597

597 **References**

598

- 599 1. **Begg, K. J., B. G. Spratt, and W. D. Donachie.** 1986. Interaction between
600 membrane proteins PBP3 and rodA is required for normal cell shape and division
601 in *Escherichia coli*. *J Bacteriol* **167**:1004-8.
- 602 2. **Blaylock, B., X. Jiang, A. Rubio, C. P. Moran, Jr., and K. Pogliano.** 2004.
603 Zipper-like interaction between proteins in adjacent daughter cells mediates
604 protein localization. *Genes Dev* **18**:2916-28.
- 605 3. **Boyle, D. S., M. M. Khattar, S. G. Addinall, J. Lutkenhaus, and W. D.**
606 **Donachie.** 1997. *ftsW* is an essential cell-division gene in *Escherichia coli*. *Mol*
607 *Microbiol* **24**:1263-73.
- 608 4. **Daniel, R. A., S. Drake, C. E. Buchanan, R. Scholle, and J. Errington.** 1994.
609 The *Bacillus subtilis* spoVD gene encodes a mother-cell-specific penicillin-binding
610 protein required for spore morphogenesis. *J Mol Biol* **235**:209-20.
- 611 5. **Datta, P., A. Dasgupta, S. Bhakta, and J. Basu.** 2002. Interaction between
612 FtsZ and FtsW of *Mycobacterium tuberculosis*. *J Biol Chem* **277**:24983-7.
- 613 6. **Datta, P., A. Dasgupta, A. K. Singh, P. Mukherjee, M. Kundu, and J. Basu.**
614 2006. Interaction between FtsW and penicillin-binding protein 3 (PBP3) directs
615 PBP3 to mid-cell, controls cell septation and mediates the formation of a trimeric
616 complex involving FtsZ, FtsW and PBP3 in mycobacteria. *Mol Microbiol* **62**:1655-
617 73.
- 618 7. **de Pedro, M. A., W. D. Donachie, J. V. Holtje, and H. Schwarz.** 2001.
619 Constitutive septal murein synthesis in *Escherichia coli* with impaired activity of
620 the morphogenetic proteins RodA and penicillin-binding protein 2. *J Bacteriol*
621 **183**:4115-26.
- 622 8. **Doan, T., K. A. Marquis, and D. Z. Rudner.** 2005. Subcellular localization of a
623 sporulation membrane protein is achieved through a network of interactions
624 along and across the septum. *Mol Microbiol* **55**:1767-81.
- 625 9. **Feilmeier, B. J., G. Iseminger, D. Schroeder, H. Webber, and G. J. Phillips.**
626 2000. Green fluorescent protein functions as a reporter for protein localization in
627 *Escherichia coli*. *J Bacteriol* **182**:4068-76.
- 628 10. **Finn, R. D., J. Mistry, B. Schuster-Bockler, S. Griffiths-Jones, V. Hollich, T.**
629 **Lassmann, S. Moxon, M. Marshall, A. Khanna, R. Durbin, S. R. Eddy, E. L.**
630 **Sonnhammer, and A. Bateman.** 2006. Pfam: clans, web tools and services.
631 *Nucleic Acids Res* **34**:D247-51.
- 632 11. **Gerard, P., T. Vernet, and A. Zapun.** 2002. Membrane topology of the
633 *Streptococcus pneumoniae* FtsW division protein. *J Bacteriol* **184**:1925-31.
- 634 12. **Green, D. W.** 2002. The bacterial cell wall as a source of antibacterial targets.
635 *Expert Opin Ther Targets* **6**:1-19.
- 636 13. **Guerout-Fleury, A. M., N. Frandsen, and P. Stragier.** 1996. Plasmids for
637 ectopic integration in *Bacillus subtilis*. *Gene* **180**:57-61.
- 638 14. **Guerout-Fleury, A. M., K. Shazand, N. Frandsen, and P. Stragier.** 1995.
639 Antibiotic-resistance cassettes for *Bacillus subtilis*. *Gene* **167**:335-6.
- 640 15. **Gutierrez, C., and J. C. Devedjian.** 1989. A plasmid facilitating in vitro
641 construction of *phoA* gene fusions in *Escherichia coli*. *Nucleic Acids Res*
642 **17**:3999.

- 643 16. **Harwood, C. R., and S. M. Cutting (ed.)**. 1990. Molecular biological methods for
644 Bacillus Wiley, New York.
- 645 17. **Henriques, A. O., H. de Lencastre, and P. J. Piggot**. 1992. A Bacillus subtilis
646 morphogene cluster that includes spoVE is homologous to the mra region of
647 Escherichia coli. *Biochimie* **74**:735-48.
- 648 18. **Henriques, A. O., P. Glaser, P. J. Piggot, and C. P. Moran, Jr.** 1998. Control of
649 cell shape and elongation by the rodA gene in Bacillus subtilis. *Mol Microbiol*
650 **28**:235-47.
- 651 19. **Holtje, J. V.** 1998. Growth of the stress-bearing and shape-maintaining murein
652 sacculus of Escherichia coli. *Microbiol Mol Biol Rev* **62**:181-203.
- 653 20. **Ikeda, M., T. Sato, M. Wachi, H. K. Jung, F. Ishino, Y. Kobayashi, and M.**
654 **Matsuhashi**. 1989. Structural similarity among Escherichia coli FtsW and RodA
655 proteins and Bacillus subtilis SpoVE protein, which function in cell division, cell
656 elongation, and spore formation, respectively. *J Bacteriol* **171**:6375-8.
- 657 21. **Ishino, F., W. Park, S. Tomioka, S. Tamaki, I. Takase, K. Kunugita, H.**
658 **Matsuzawa, S. Asoh, T. Ohta, B. G. Spratt, and et al.** 1986. Peptidoglycan
659 synthetic activities in membranes of Escherichia coli caused by overproduction of
660 penicillin-binding protein 2 and rodA protein. *J Biol Chem* **261**:7024-31.
- 661 22. **Joris, B., G. Dive, A. Henriques, P. J. Piggot, and J. M. Ghuyssen**. 1990. The
662 life-cycle proteins RodA of Escherichia coli and SpoVE of Bacillus subtilis have
663 very similar primary structures. *Mol Microbiol* **4**:513-7.
- 664 23. **Karimova, G., N. Dautin, and D. Ladant**. 2005. Interaction network among
665 Escherichia coli membrane proteins involved in cell division as revealed by
666 bacterial two-hybrid analysis. *J Bacteriol* **187**:2233-43.
- 667 24. **Karmazyn-Campelli, C., C. Bonamy, B. Savelli, and P. Stragier**. 1989.
668 Tandem genes encoding sigma-factors for consecutive steps of development in
669 Bacillus subtilis. *Genes Dev* **3**:150-7.
- 670 25. **Karow, M. L., and P. J. Piggot**. 1995. Construction of gusA transcriptional fusion
671 vectors for Bacillus subtilis and their utilization for studies of spore formation.
672 *Gene* **163**:69-74.
- 673 26. **Khattar, M. M., S. G. Addinall, K. H. Stedul, D. S. Boyle, J. Lutkenhaus, and**
674 **W. D. Donachie**. 1997. Two polypeptide products of the Escherichia coli cell
675 division gene ftsW and a possible role for FtsW in FtsZ function. *J Bacteriol*
676 **179**:784-93.
- 677 27. **Khattar, M. M., K. J. Begg, and W. D. Donachie**. 1994. Identification of FtsW
678 and characterization of a new ftsW division mutant of Escherichia coli. *J Bacteriol*
679 **176**:7140-7.
- 680 28. **Lara, B., and J. A. Ayala**. 2002. Topological characterization of the essential
681 Escherichia coli cell division protein FtsW. *FEMS Microbiol Lett* **216**:23-32.
- 682 29. **Lara, B., D. Mengin-Lecreulx, J. A. Ayala, and J. van Heijenoort**. 2005.
683 Peptidoglycan precursor pools associated with MraY and FtsW deficiencies or
684 antibiotic treatments. *FEMS Microbiol Lett* **250**:195-200.
- 685 30. **Lemon, K. P., and A. D. Grossman**. 2000. Movement of replicating DNA
686 through a stationary replisome. *Mol Cell* **6**:1321-30.

- 687 31. **Levin, P. A., and R. Losick.** 1996. Transcription factor Spo0A switches the
688 localization of the cell division protein FtsZ from a medial to a bipolar pattern in
689 *Bacillus subtilis*. *Genes Dev* **10**:478-88.
- 690 32. **Mallidis, C. G., and J. Scholefield.** 1987. Relation of the heat resistance of
691 bacterial spores to chemical composition and structure. II. Relation to cortex and
692 structure. *J Appl Bacteriol* **63**:207-15.
- 693 33. **Manoil, C.** 1991. Analysis of membrane protein topology using alkaline
694 phosphatase and beta-galactosidase gene fusions. *Methods Cell Biol* **34**:61-75.
- 695 34. **Matsushashi, M.** 1994. Utilization of lipid-linked precursors and the formation of
696 peptidoglycan in the process of cell growth and division: membrane enzymes
697 involved in the final steps of peptidoglycan synthesis and mechanism of their
698 regulation. *In* J.-M. Ghuysen and R. Hackenbeck (ed.), *Bacterial Cell Wall*.
699 Elsevier, Amsterdam.
- 700 35. **Miller, J. H.** 1992. *A short course in bacterial genetics : a laboratory manual and*
701 *handbook for Escherichia coli and related bacteria* Cold Spring Harbor
702 Laboratory Press, Plainview, NY.
- 703 36. **Pastoret, S., C. Fraipont, T. den Blaauwen, B. Wolf, M. E. Aarsman, A.**
704 **Piette, A. Thomas, R. Brasseur, and M. Nguyen-Disteche.** 2004. Functional
705 analysis of the cell division protein FtsW of *Escherichia coli*. *J Bacteriol*
706 **186**:8370-9.
- 707 37. **Piggot, P. J., K. F. Chak, and U. D. Bugaichuk.** 1986. Isolation and
708 characterization of a clone of the spoVE locus of *Bacillus subtilis*. *J Gen Microbiol*
709 **132**:1875-81.
- 710 38. **Piggot, P. J., and J. G. Coote.** 1976. Genetic aspects of bacterial endospore
711 formation. *Bacteriol Rev* **40**:908-62.
- 712 39. **Pogliano, J., N. Osborne, M. D. Sharp, A. Abanes-De Mello, A. Perez, Y. L.**
713 **Sun, and K. Pogliano.** 1999. A vital stain for studying membrane dynamics in
714 bacteria: a novel mechanism controlling septation during *Bacillus subtilis*
715 sporulation. *Mol Microbiol* **31**:1149-59.
- 716 40. **Popham, D. L.** 2002. Specialized peptidoglycan of the bacterial endospore: the
717 inner wall of the lockbox. *Cell Mol Life Sci* **59**:426-33.
- 718 41. **Real, G., S. Autret, E. J. Harry, J. Errington, and A. O. Henriques.** 2005. Cell
719 division protein DivIB influences the Spo0J/Soj system of chromosome
720 segregation in *Bacillus subtilis*. *Mol Microbiol* **55**:349-67.
- 721 42. **Real, G., and A. O. Henriques.** 2006. Localization of the *Bacillus subtilis* murB
722 gene within the dcw cluster is important for growth and sporulation. *J Bacteriol*
723 **188**:1721-32.
- 724 43. **Rudner, D. Z., Q. Pan, and R. M. Losick.** 2002. Evidence that subcellular
725 localization of a bacterial membrane protein is achieved by diffusion and capture.
726 *Proc Natl Acad Sci U S A* **99**:8701-6.
- 727 44. **Schuster-Bockler, B., J. Schultz, and S. Rahmann.** 2004. HMM Logos for
728 visualization of protein families. *BMC Bioinformatics* **5**:7.
- 729 45. **Seyler, R. W., Jr., A. O. Henriques, A. J. Ozin, and C. P. Moran, Jr.** 1997.
730 Assembly and interactions of cotJ-encoded proteins, constituents of the inner
731 layers of the *Bacillus subtilis* spore coat. *Mol Microbiol* **25**:955-66.

- 732 46. **Shapiro, L., H. H. McAdams, and R. Losick.** 2002. Generating and exploiting
733 polarity in bacteria. *Science* **298**:1942-6.
- 734 47. **Smith, C. A.** 2006. Structure, function and dynamics in the mur family of bacterial
735 cell wall ligases. *J Mol Biol* **362**:640-55.
- 736 48. **Sterlini, J. M., and J. Mandelstam.** 1969. Commitment to sporulation in *Bacillus*
737 *subtilis* and its relationship to development of actinomycin resistance. *Biochem J*
738 **113**:29-37.
- 739 49. **Theeragool, G., A. Miyao, K. Yamada, T. Sato, and Y. Kobayashi.** 1993. In
740 vivo expression of the *Bacillus subtilis* spoVE gene. *J Bacteriol* **175**:4071-80.
- 741 50. **van Dam, V., R. Sijbrandi, M. Kol, E. Swiezewska, B. de Kruijff, and E.**
742 **Breukink.** 2007. Transmembrane transport of peptidoglycan precursors across
743 model and bacterial membranes. *Mol Microbiol* **64**:1105-14.
- 744 51. **van Heijenoort, J.** 2001. Recent advances in the formation of the bacterial
745 peptidoglycan monomer unit. *Nat Prod Rep* **18**:503-19.
- 746 52. **van Ooij, C., P. Eichenberger, and R. Losick.** 2004. Dynamic patterns of
747 subcellular protein localization during spore coat morphogenesis in *Bacillus*
748 *subtilis*. *J Bacteriol* **186**:4441-8.
- 749 53. **van Ooij, C., and R. Losick.** 2003. Subcellular localization of a small sporulation
750 protein in *Bacillus subtilis*. *J Bacteriol* **185**:1391-8.
- 751 54. **Vasudevan, P., A. Weaver, E. D. Reichert, S. D. Linnstaedt, and D. L.**
752 **Popham.** 2007. Spore cortex formation in *Bacillus subtilis* is regulated by
753 accumulation of peptidoglycan precursors under the control of sigma K. *Mol*
754 *Microbiol* **65**:1582-94.
- 755 55. **von Heijne, G.** 1992. Membrane protein structure prediction. Hydrophobicity
756 analysis and the positive-inside rule. *J Mol Biol* **225**:487-94.
- 757 56. **Warth, A. D., and J. L. Strominger.** 1972. Structure of the peptidoglycan from
758 spores of *Bacillus subtilis*. *Biochemistry* **11**:1389-96.
- 759 57. **Warth, A. D., and J. L. Strominger.** 1969. Structure of the peptidoglycan of
760 bacterial spores: occurrence of the lactam of muramic acid. *Proc Natl Acad Sci U*
761 *S A* **64**:528-35.
- 762 58. **Wickus, G. G., A. D. Warth, and J. L. Strominger.** 1972. Appearance of
763 muramic lactam during cortex synthesis in sporulating cultures of *Bacillus cereus*
764 and *Bacillus megaterium*. *J Bacteriol* **111**:625-7.
- 765 59. **Youngman, P., J. B. Perkins, and R. Losick.** 1984. A novel method for the
766 rapid cloning in *Escherichia coli* of *Bacillus subtilis* chromosomal DNA adjacent to
767 Tn917 insertions. *Mol Gen Genet* **195**:424-33.
- 768
769
770

770 **Tables**771 **Table 1.** Bacterial strains.

772

773	Strain	Genotype	Origin/reference
774			
775	MB24	<i>trpC2 metC3</i>	Laboratory stock
776	SL666	<i>spoVE85</i>	(38)
777	AH3561	<i>spoVE85 amyE::spoVE-yfp</i>	This work
778	AH3700	<i>spoVE85 amyE::spoVEI58N-yfp</i>	This work
779	AH3701	<i>spoVE85 amyE::spoVEC82R-yfp</i>	This work
780	AH3702	<i>spoVE85 amyE::spoVES103N-yfp</i>	This work
781	AH3703	<i>spoVE85 amyE::spoVEE126G-yfp</i>	This work
782	AH3704	<i>spoVE85 amyE::spoVEC160R-yfp</i>	This work
783	AH3705	<i>spoVE85 amyE::spoVEG292R-yfp</i>	This work
784	AH3706	<i>spoVE85 amyE::spoVEG355D-yfp</i>	This work
785	PY79	wild-type	(59)
786	JDB223	<i>ftsW::ftsW-gfpΩspc</i>	This work
787	JDB646	<i>spoVE::neo</i>	P. Eichenberger
788	JDB1376	<i>spoVE::neo amyE::P_{spoVE}-spoVE-cfpΩcat</i>	This work
789	JDB1407	<i>amyE::P_{spoVE}-ftsW-gfpΩcat</i>	This work
790	JDB1483	<i>amyE::P_{spoVE}-P_{ftsW(102)}-spoVE-gfpΩcat</i>	This work
791	JDB1678	<i>spoVE::neo ftsW-yfpΩspc amyE::P_{spoVE}-spoVE-cfpΩcat</i>	This work
792	JDB1752	Δ <i>spoVE::tet</i>	This work
793	JDB1755	<i>spoVE::neo amyE::P_{spoVE}-ftsW-gfpΩcat</i>	This work
794	JDB1813	Δ <i>spoVE::tet amyE::P_{spoVE}-spoVE-gfpΩcm</i>	This work
795	JDB1835	Δ <i>spoVE::tet amyE::P_{spoVE}-spoVE-gfpΩspcΩcat</i>	This work
796	JDB1845	Δ <i>spoVE::tet amyE::P_{spoVE}-spoVEG335-gfpΩspcΩcat</i>	This work
797	JDB1846	Δ <i>spoVE::tet amyE::P_{spoVE}-spoVES341A-gfpΩspcΩcat</i>	This work
798	JDB1847	Δ <i>spoVE::tet amyE::P_{spoVE}-spoVEG343A-gfpΩspcΩcat</i>	This work
799	JDB1848	Δ <i>spoVE::tet amyE::P_{spoVE}-spoVEN322A-gfpΩspcΩcat</i>	This work
800	JDB1849	Δ <i>spoVE::tet amyE::P_{spoVE}-spoVEE271A-gfpΩspcΩcat</i>	This work
801	JDB1850	Δ <i>spoVE::tet amyE::P_{spoVE}-spoVEW69A-gfpΩcat</i>	This work
802	JDB1851	Δ <i>spoVE::tet amyE::P_{spoVE}-spoVEK76A-gfpΩcat</i>	This work
803	JDB1852	Δ <i>spoVE::tet amyE::P_{spoVE}-spoVET173A-gfpΩcat</i>	This work
804	JDB1853	Δ <i>spoVE::tet amyE::P_{spoVE}-spoVE-gfpΩcat</i>	This work
805	JDB1854	Δ <i>spoVE::tet amyE::P_{spoVE}-spoVEI58N-yfpΩcat</i>	This work
806	JDB1855	Δ <i>spoVE::tet amyE::P_{spoVE}-spoVEC82R-yfpΩcat</i>	This work
807	JDB1856	Δ <i>spoVE::tet amyE::P_{spoVE}-spoVES103N-yfpΩcat</i>	This work
808	JDB1857	Δ <i>spoVE::tet amyE::P_{spoVE}-spoVEE116G-yfpΩcat</i>	This work
809	JDB1858	Δ <i>spoVE::tet amyE::P_{spoVE}-spoVEC160R-yfpΩcat</i>	This work
810	JDB1859	Δ <i>spoVE::tet amyE::P_{spoVE}-spoVEG292R-yfpΩcat</i>	This work
811	JDB1860	Δ <i>spoVE::tet amyE::P_{spoVE}-spoVEG355D-yfpΩcat</i>	This work

812	JDB1926	$\Delta spoVE::tet amyE::P_{spoVE}-spoVEG335A-gfp\Omega cat$	This work
813	JDB1927	$\Delta spoVE::tet amyE::P_{spoVE}-spoVES341A-gfp\Omega cat$	This work
814	JDB1928	$\Delta spoVE::tet amyE::P_{spoVE}-spoVEG343A-gfp\Omega cat$	This work
815	JDB1929	$\Delta spoVE::tet amyE::P_{spoVE}-spoVEN322A-gfp\Omega cat$	This work
816	JDB1930	$\Delta spoVE::tet amyE::P_{spoVE}-spoVEE271A-gfp\Omega cat$	This work
817	JDB1933	$\Delta spoVE::tet amyE::P_{spoVE}-spoVE-gfp\Omega cat$	This work
818			

ACCEPTED

818 **Table 2.** Phenotypes of SpoVE mutants.*

819

Genotype	CFU/ml pre-heat	CFU/ml post-heat	Percent sporulation	Accumulation ²	Localization Ratio ³	Localization ⁴
Wildtype (PY79)	1.9x10 ⁸	1.4x10 ⁸	74	N/A	N/A	N/A
<i>ΔspoVE::tet</i>	8.8x10 ⁷	0	0	N/A	N/A	N/A
<i>spoVE-gfp</i>	2.1x10 ⁸	1.4x10 ⁸	67	++++	3.51 ± 0.20	OFM
<i>spoVEG335A-gfp</i>	1.3x10 ⁸	0	0	++++	3.34 ± 0.21	OFM
<i>spoVES341A-gfp</i>	1.6x10 ⁸	0	0	+++++	3.32 ± 0.33	OFM
<i>spoVEG343A-gfp</i>	1.2x10 ⁸	0	0	+++++	3.28 ± 0.19	OFM
<i>spoVEN322A-gfp</i>	9.9x10 ⁷	1.6x10 ⁵	0.16	+++++	3.20 ± 0.12	OFM
<i>spoVEE271A-gfp</i>	1.2x10 ⁸	0	0	+++++	3.11 ± 0.22	OFM
<i>spoVEI58N-yfp</i>	2.6x10 ⁸	0	0	++	nd	OFM
<i>spoVEC82R-yfp</i>	3.0x10 ⁸	0	0	nd	nd	nd
<i>spoVES103N-yfp</i>	2.5x10 ⁸	0	0	+++++	nd	OFM
<i>spoVEE116G-yfp</i>	1.4x10 ⁸	0	0	+++++	nd	OFM
<i>spoVEC160R-yfp</i>	9.2x10 ⁷	0	0	+	nd	nd
<i>spoVEG292R-yfp</i>	1.3x10 ⁸	0	0	++	nd	MCM
<i>spoVEG355D-yfp</i>	1.6x10 ⁸	0	0	+	nd	MCM
<i>spoVEW69A-gfp</i>	1.0x10 ⁸	6.0x10 ¹	0.00006	++	1.97 ± 0.15	MCM
<i>spoVEK76A-gfp</i>	7.3x10 ⁷	3.8x10 ²	0.0005	++	1.94 ± 0.13	MCM
<i>spoVET173A-gfp</i>	9.7x10 ⁷	1.8x10 ²	0.0002	++	1.89 ± 0.28	MCM

820

821 ¹Data represents one typical heat kill experiment. Each strain was grown in DSM for 24h
822 at 37C, then exposed to 80°C for 20 min.

823

824 ²SpoVE-GFP or SpoVE-YFP accumulation at hour 6 of sporulation. nd, not detectable.

825

826 ³Ratio between all 4 mother cell membranes (including forespore) and the 2 sporangial
827 cell membranes. See text for details and figure 5.

828

829 ⁴SpoVE localization as assessed by GFP and YFP fusions. See figure 5. N/A, not
830 assessed. OFM, outer forespore membrane. MCM, Mother cell membranes.

831

831

832 **Table 3.** Description and enzyme activities of SpoVE'-PhoA and SpoVE'-LacZ fusion
833 proteins.

834

835

836	Last SpoVE residue	PhoA activity	LacZ activity
837		Rel. Units	Rel. Units ⁺
838			
839	D40	117.1	12.3
840	K76	62.9	261.0
841	G106	534.5	10.1
842	P146	2.16	228.5
843	P162	117.2	8.9
844	S205	96.56	11.5
845	F228	244.8	7.9
846	T262	88.5	27.7
847	P300	23.6	463.1
848	Y366	11.5	398.1

849

850 *The relative units (Rel. U) of phosphatase activity were calculated as described (33).

851 *The relative units (Rel. U) of β -galactosidase activity were calculated as described (35).

852

853

854

854 **Figure Legends**

855

856 **Figure 1. SpoVE-YFP localization throughout sporulation. A.** Strain AH3561857 (*spoVE85 amyE::spoVE-yfp*) was induced to sporulate in DSM medium and samples

858 were collected at the onset (T0) and throughout sporulation and labeled with vital stain

859 FM4-64 for visualization of membranes by fluorescence microscopy. The first column

860 shows phase contrast images, the second column depicts the co-localization of the

861 membranes (red) and the YFP signal (yellow). The third column shows the localization of

862 SpoVE-YFP alone (yellow). Scale bar (white) is 1 μm . **B.** Strain JDB1813 carrying a

863 SpoVE-GFP fusion was visualized by time-lapse microscopy every 7 min as it proceeded

864 through sporulation. Shown is a single cell with images taken at five consecutive time

865 points (a, t = 0; b, t = 7 min; c, t = 14 min; d, t = 21 min; e, t = 28 min).

866

867 **Figure 2. Localization of SpoVE-GFP and FtsW-GFP. A.** Strains JDB223 (a-d;868 *ftsW::ftsW-gfp*), JDB1755 (e-h; *spoVE::neo amyE::P_{spoVE}-ftsW-gfp*), JDB1483 (i-l;869 *amyE::P_{spoVE}-P_{ftsW(102)}}-spoVE-gfp*), and JDB1835 (m-p; $\Delta spoVE::tet amyE::P_{spoVE}}-spoVE-$ 870 *gfp*) were grown in CH medium and samples taken before resuspension at OD600 = 0.5

871 (“vegetative”; a, b, e, f, i, j, m, n) or at T3 of sporulation in A+B medium (“sporulation

872 (T3”); c, d, g, h, k, l, o, p) and observed by fluorescence microscopy. Cells were labeled

873 with FM4-64 to visualize membranes. The first and third columns show GFP signal; the

874 second and fourth columns show overlay of GFP and membrane signals. Scale bar

875 (white) is 1 μm . **B, C.** Strains JDB223 (*ftsW::ftsW-gfp*) and JDB1755 (*spoVE::neo*876 *amyE::P_{spoVE}-ftsW-gfp*) were induced to sporulate by resuspension and samples were

877 collected at the onset of sporulation (T0) and subsequently at hourly intervals. Samples

878 were resolved using a 12% SDS-PAGE gel and subjected to immunoblot analysis with an
879 anti-GFP antibody.

880

881 **Figure 3. Fluorescence microscopy of FtsW and SpoVE.** Strain JDB1678 (*ftsW-yfp*,
882 *spoVE::neo*, *amyE::spoVE-cfp*) was sporulated by resuspension, T is in minutes. Cells
883 were labeled with FM4-64 to visualize membranes. Consecutive images were acquired
884 using YFP, CFP and FM4-64 filter sets. The overlay was generated using the Nikon NIS
885 program from the YFP, CFP, and FM4-64 images. Measurement of pixel intensities was
886 performed using the Line Scan function of the Nikon NIS program. The values for the CFP
887 and YFP channels are plotted as a function of distance along the arrow shown in the
888 overlay. Note that different scales were used for different samples; scale bar (white) is 1
889 μm .

890 **Figure 4. Topology model for *B. subtilis* SpoVE and localization of point mutations.**

891 **A.** *B. subtilis* SpoVE membrane topology and the location of SpoVE mutations. The
892 beginning and end of each transmembrane segment (TM I to X) is indicated by the
893 residue number. The model is derived from TopPredII predictions (55) and LacZ and
894 PhoA fusion analysis. SpoVE mutations are coded according to how SpoVE-GFP or
895 SpoVE-YFP mutant proteins carrying the respective mutations accumulate and localize
896 during sporulation: green (reduced accumulation); red (accumulate and localize); and blue
897 (accumulate but are mislocalized). **B.** Partial alignment of SEDS proteins (SpoVE, FtsW
898 and RodA) from selected members of the genus *Bacillus*. The alignment shows parts of
899 TM II, III, VI and X (as represented in panel A for the *B. subtilis* SpoVE protein) and was

900 obtained using CLUSTAL-W (www.ebi.ac.uk). SpoVE mutations W69A, K76, C82R and
901 T173A are in residues conserved only among predicted SpoVE proteins, whereas
902 mutations G335A, S341A and G343A are in conserved residues among the *Bacillus spp.*
903 SEDS proteins. Residues in the position corresponding to all 6 mutations are shown
904 against a yellow background. Other conserved residues in TM X are shown in red. *Bs*, *B.*
905 *subtilis*; *Bl*, *B. licheniformis*; *Bamy*, *B. amyloliquefaciens*; *Bth*, *B. thuringiensis*; *Bcer*, *B.*
906 *cereus*; *Bcl*, *B. clausii*; *Banth*, *B. anthracis*.

907

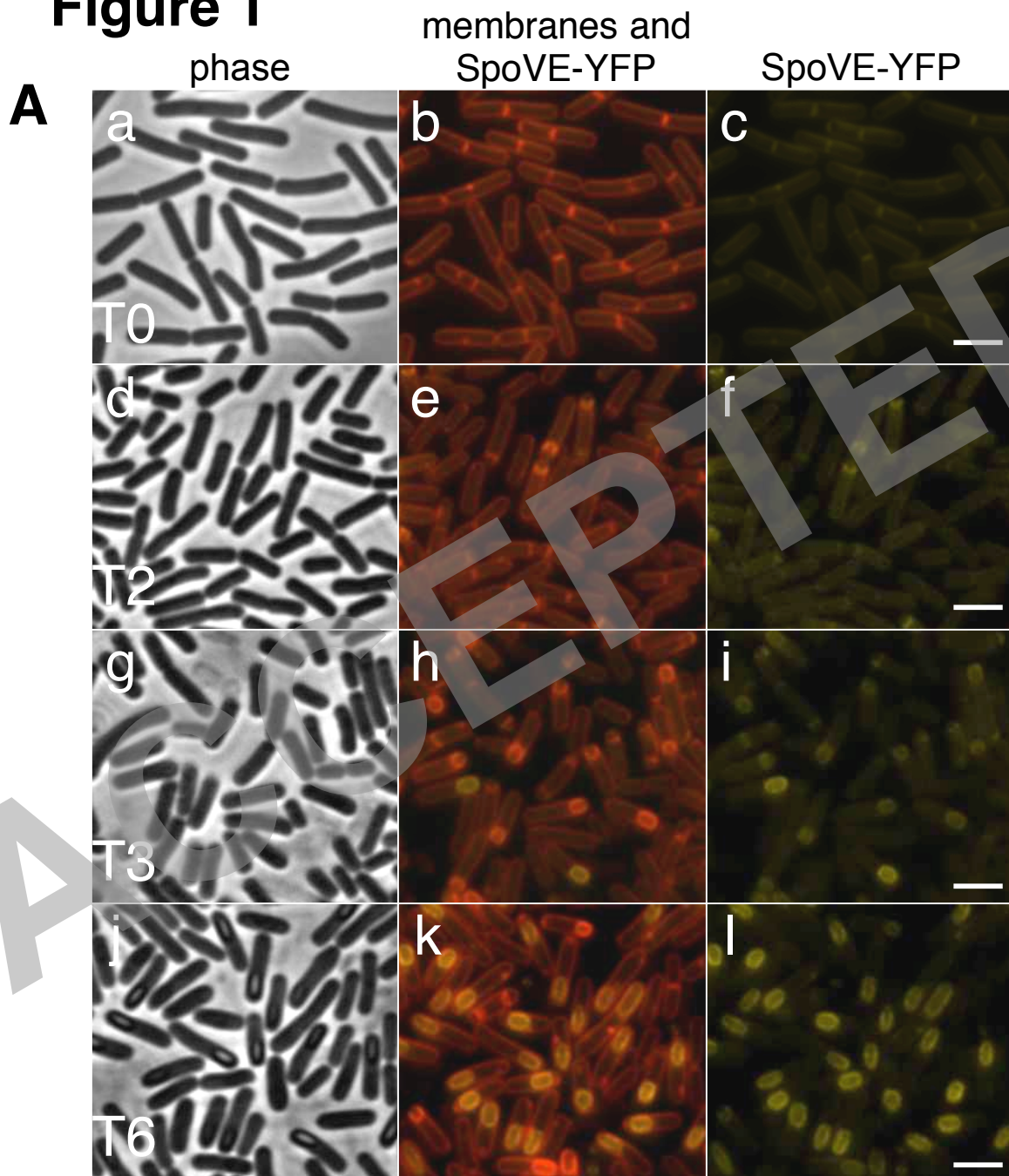
908 **Figure 5. Fluorescence microscopy of *spoVE* point mutants. A.** Strains expressed
909 either wild-type SpoVE-GFP (JDB1835) or SpoVE-GFP mutants generated using site
910 directed mutagenesis: G335A (JDB1845), S341A (JDB1846), G343A (JDB1847), N322A
911 (JDB1848), E271A (JDB1849), W69A (JDB1850), K76A (JDB1851), and T173A
912 (JDB1852). Scale bar (yellow) is 1 μ m. **B.** Strains expressed wild type SpoVE-YFP
913 (JDB1853) or SpoVE-YFP mutants generated by random mutagenesis: I58N (JDB1854),
914 C82R (JDB1855), S103N (JDB1856), E116G (JDB1857), C160R (JDB1858), G292R
915 (JDB1859), and G355D (JDB1860). **C.** We quantified SpoVE localization using ImageJ
916 (NIH) to measure the average pixel intensity for five lines spanning the forespore (red)
917 and for five lines across the cell at the other end (blue). When the red:blue ratio is 2, then
918 GFP signal is evenly distributed in all membranes (left). When the red:blue ratio is >2, the
919 GFP signal is concentrated at the forespore (right). All strains were sporulated by
920 resuspension, cells were labeled by FM4-64 and samples for microscopy were obtained
921 at T2.5.

922

923 **Figure 6. Accumulation of mutant SpoVE proteins during sporulation. A.** Strains
 924 were induced to sporulate in DSM medium and collected 6 h after the onset of sporulation
 925 for western-blot analysis using an anti-GFP antibody. wt: *spoVE85 amyE::spoVE-yfp*
 926 (AH3561); C160R: *spoVE85 amyE::spoVEC160R-yfp* (AH3704); C82R: *spoVE85*
 927 *amyE::spoVEC82R-yfp* (AH3701); S103N: *spoVE85 amyE::spoVES103N-yfp* (AH3702);
 928 E126G: *spoVE85 amyE::spoVEE126G-yfp* (AH3703); I59N: *spoVE85 amyE::spoVEI59N-*
 929 *yfp* (AH3700); G292R: *spoVE85 amyE::spoVEG292R-yfp* (AH3705); G355D: *spoVE85*
 930 *amyE::spoVEG355D-yfp* (AH3706); no YFP: *spoVE* wt (MB24). **B.** Strains were
 931 sporulated by resuspension and collected at T3 of sporulation for western-blot analysis
 932 using an anti-GFP antibody. wt: $\Delta spoVE::tet amyE::P_{spoVE}-spoVE-gfp$ (JDB1835); G335A:
 933 $\Delta spoVE::tet amyE::P_{spoVE}-spoVE(G335A)-gfp$ (JDB1845); S341A: $\Delta spoVE::tet$
 934 *amyE::P_{spoVE}-spoVE(S341A)-gfp* (JDB1846); G343A: ($\Delta spoVE::tet amyE::P_{spoVE}-$
 935 *spoVE(G343A)-gfp* (JDB1847); N322A: $\Delta spoVE::tet amyE::P_{spoVE}-spoVE(N322A)-gfp$
 936 (JDB1848); E271A: $\Delta spoVE::tet amyE::P_{spoVE}-spoVE(E271A)-gfp$ (JDB1849); W69A:
 937 ($\Delta spoVE::tet amyE::P_{spoVE}-spoVE(W69A)-gfp$ (JDB1850); K76A: $\Delta spoVE::tet amyE::P_{spoVE}-$
 938 *spoVE(K76A)-gfp* (JDB1851); T173A: $\Delta spoVE::tet amyE::P_{spoVE}-spoVE(T173A)-gfp$
 939 (JDB1852).

940 **Supplementary Figure 1. (Top)** Topological model for SpoVE. **(Bottom)** Partial
 941 alignment of SEDS proteins (SpoVE, FtsW and RodA) from selected members of the
 942 genus *Bacillus*. The alignment shows parts of TM II, IV, V, IX and X as well as outer loops
 943 OL II and IV (as represented in Figure 4 panel A for the *B. subtilis* SpoVE protein) and
 944 was obtained using CLUSTAL-W (www.ebi.ac.uk). SpoVE mutations E116G, E271A and

Figure 1



B

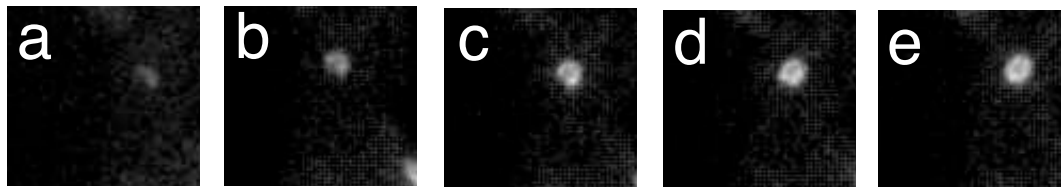
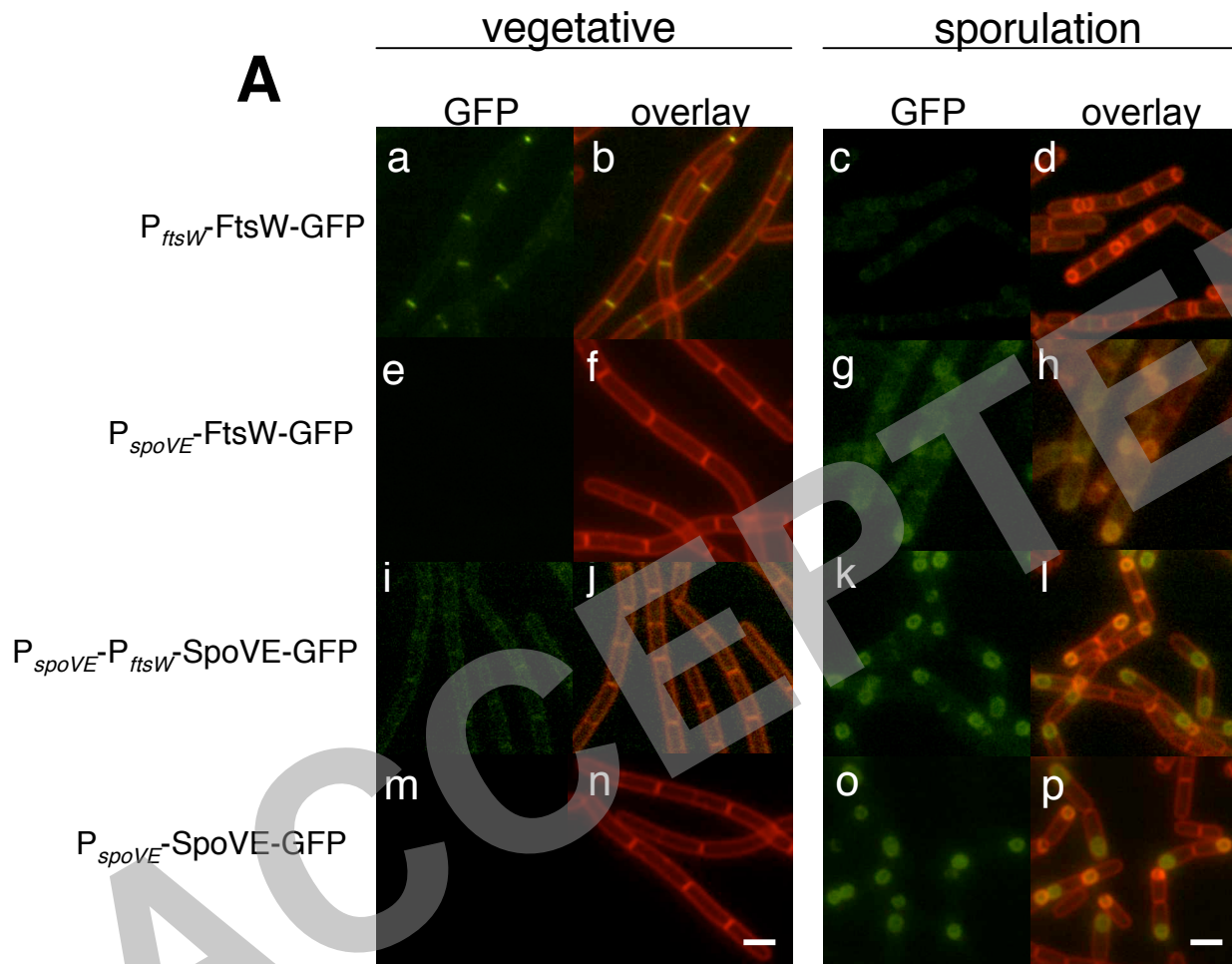
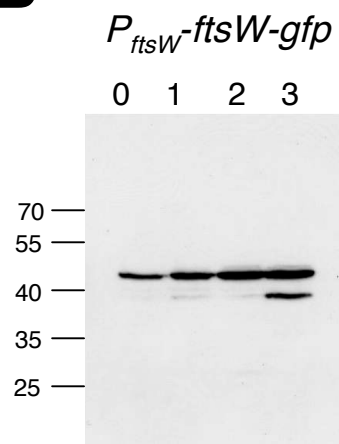


Figure 2



B



C

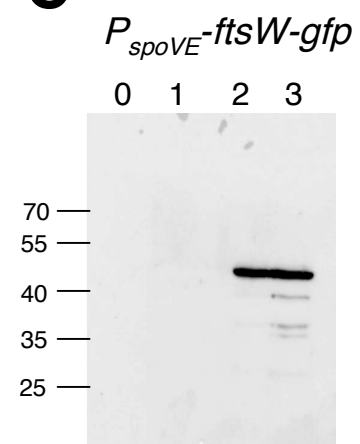


Figure 3

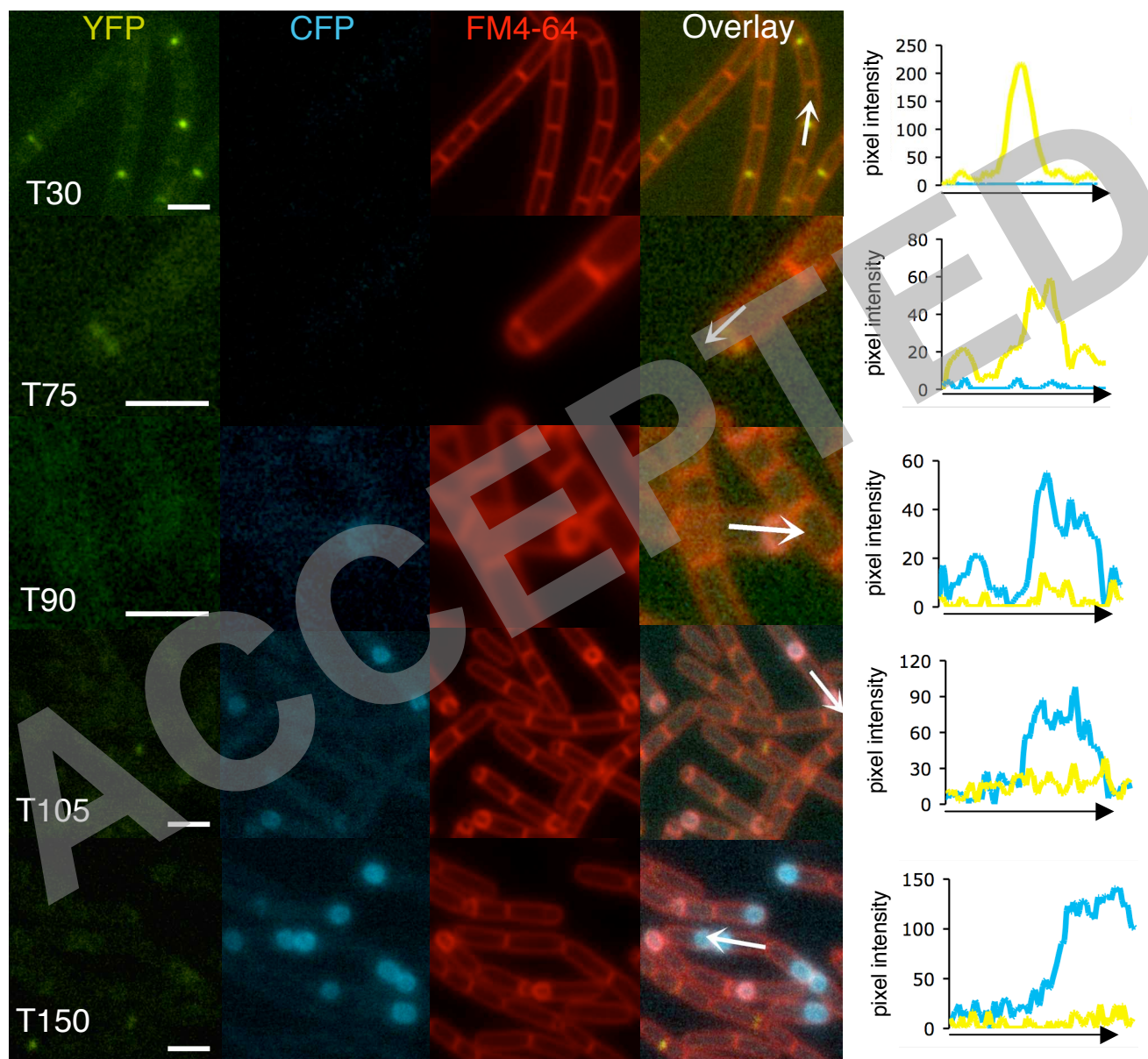
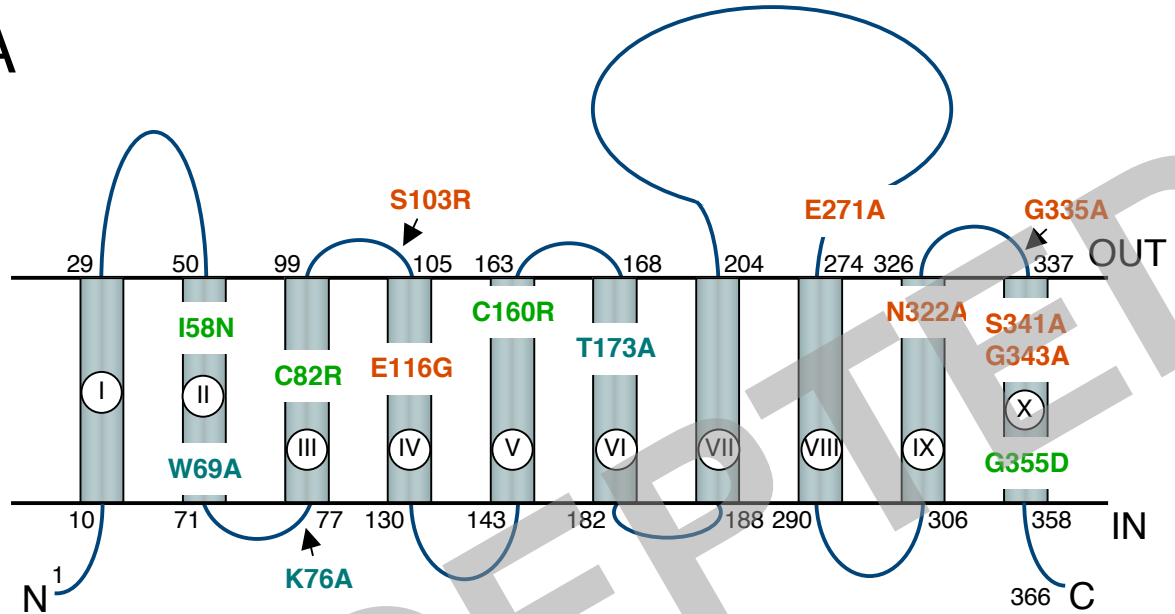


Figure 4

A



B

	69	76	82	173	335	341	343
RodA	NVDY W TWRT	K LLMV I CFLL	VMVGT C IVM	VT G ITLPFL S Y G GSSL		
FtsW	NVDY W TWRT	K LL I IV C FLL	VMVGT C IIM	VT G ITLPFL S Y G GSSL		
SpoVE	NVDY W TWRT	K LL L I I CFLL	VMVGT C IIM	VT G ITLPFL S Y G GSSL		
Bs	KIDY W VWRT	K VILLV C FILL	VMVGT C IIM	VT G ITLPFL S Y G GSSL		
Bl	KIDY W VWRT	K VILLV C FILL	VMVGT C IIM	VT G ITLPFL S Y G GSSL		
Bamy	RLDY W VWRT	K ILLI V C F ALL	VMVGT C TVM	VT G ITLP L L S Y G GSSL		
Bth	KIDY W VWRT	K VILLV C FILL	VMVGT C IIM	VT G ITLPFL S Y G GSSL		
Bcl	LFYKALAH	FQKGILLVSVL	IIGLIA T CM	IT G V T LP F I S Y G GSSL		
Banth	LFYKAFAN	FQK F LL L ISV V	I I AL I AL C I	LT G V T LP F I S Y G GSSL		
Bs	VFPYK V FAH	I Q K F ILLAS V A	I I GL I A F CV	IT G V P LP F I S Y G G S SM		
Bl	VVPYK F WRK	V L AAMGL G G I G	L I GG T V L IM	LT G V P LP F I S Y G GSSL		
Bamy	LVD F DL F RN	I P VYA I GM V LL	V I GS V I A TM	IT G L A LP F I S Y G G S AL		
Bth	I V PYK F WRK	V L AAMGL G G I G	L I GG T V L IM	LT G V P LP F I S Y G GSSL		
Bcl	YFDLE Q LEK	L Y FI I GI L SL	IC F F I V L VM	VT G I P LL F V S Y G G S ST		
Banth	YFDLE Q LEK	I Y I Y LF G I L SL	IC F FF V A V M	VT G V P LL F I S Y G G S SV		
Bs	YFDLE Q LEK	L Y V L I A GV L SL	IC F F I V M VM	VT G I P LL F V S Y G G S SV		
Bl	SIDLD Q LQK	W P LY I AG F ASL	L Y AA A I A CI	V K G I A LP F L S Y G G S SL		
Bamy	SIDLD Q LQK	W P LY I AG F ASL	L Y AA A I A CI	V K G I A LP F L S Y G G S SL		
Bth	LVDY E YLKR	I P I F AF G M I LL	V L V V I I ATA	VT G I A LP F L S Y G G S SAL		
Bcl	SIDLD Q LQK	W P LY I AG F ASL	L Y AA A I A CI	V K G I A LP F L S Y G G S SL		
Banth	SIDLD Q LQK	W P LY I AG F ASL	L Y AA A I A CI	V K G I A LP F L S Y G G S SL		

TM II
TM III
TM VI
TM X

Figure 5

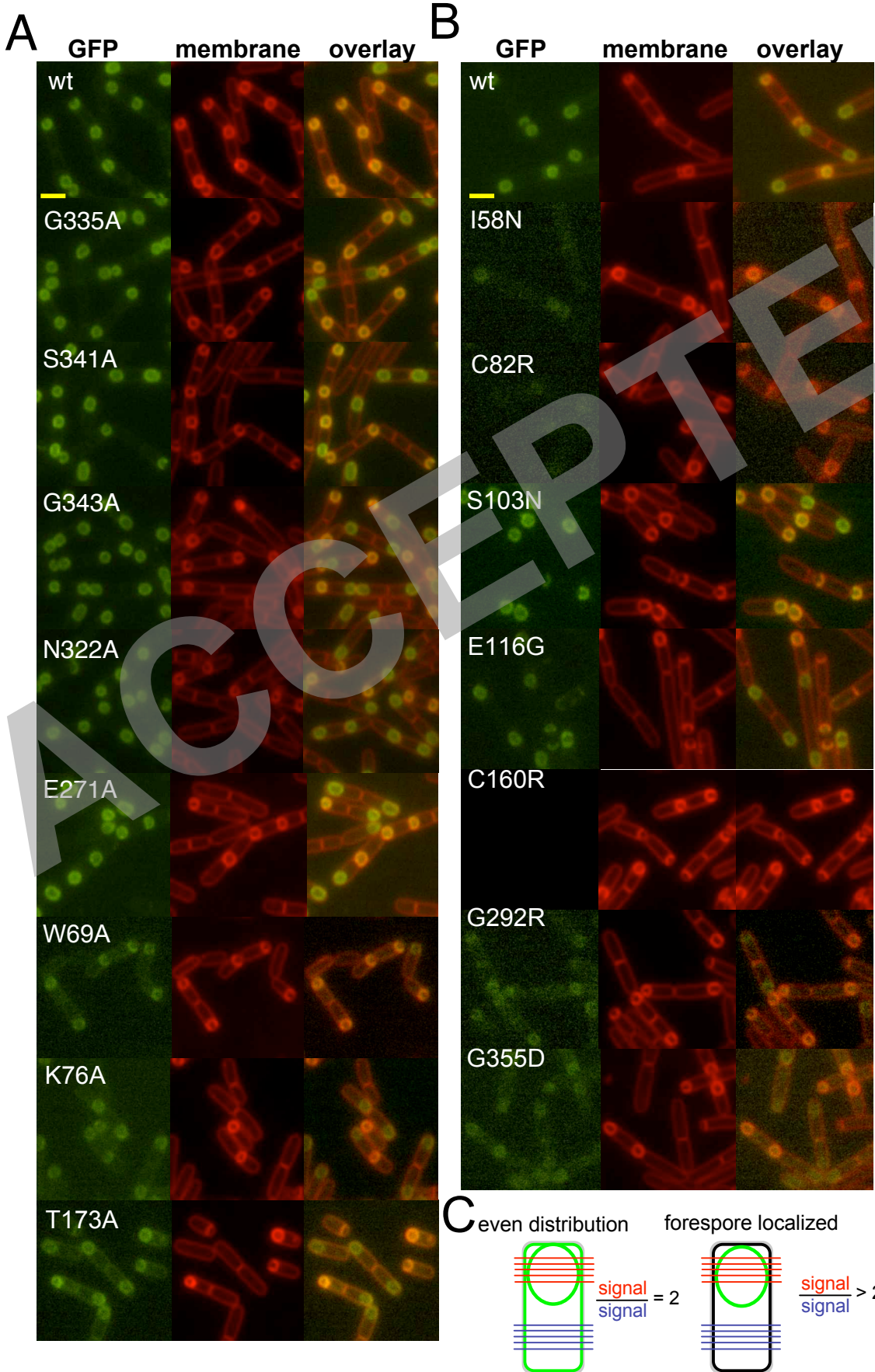
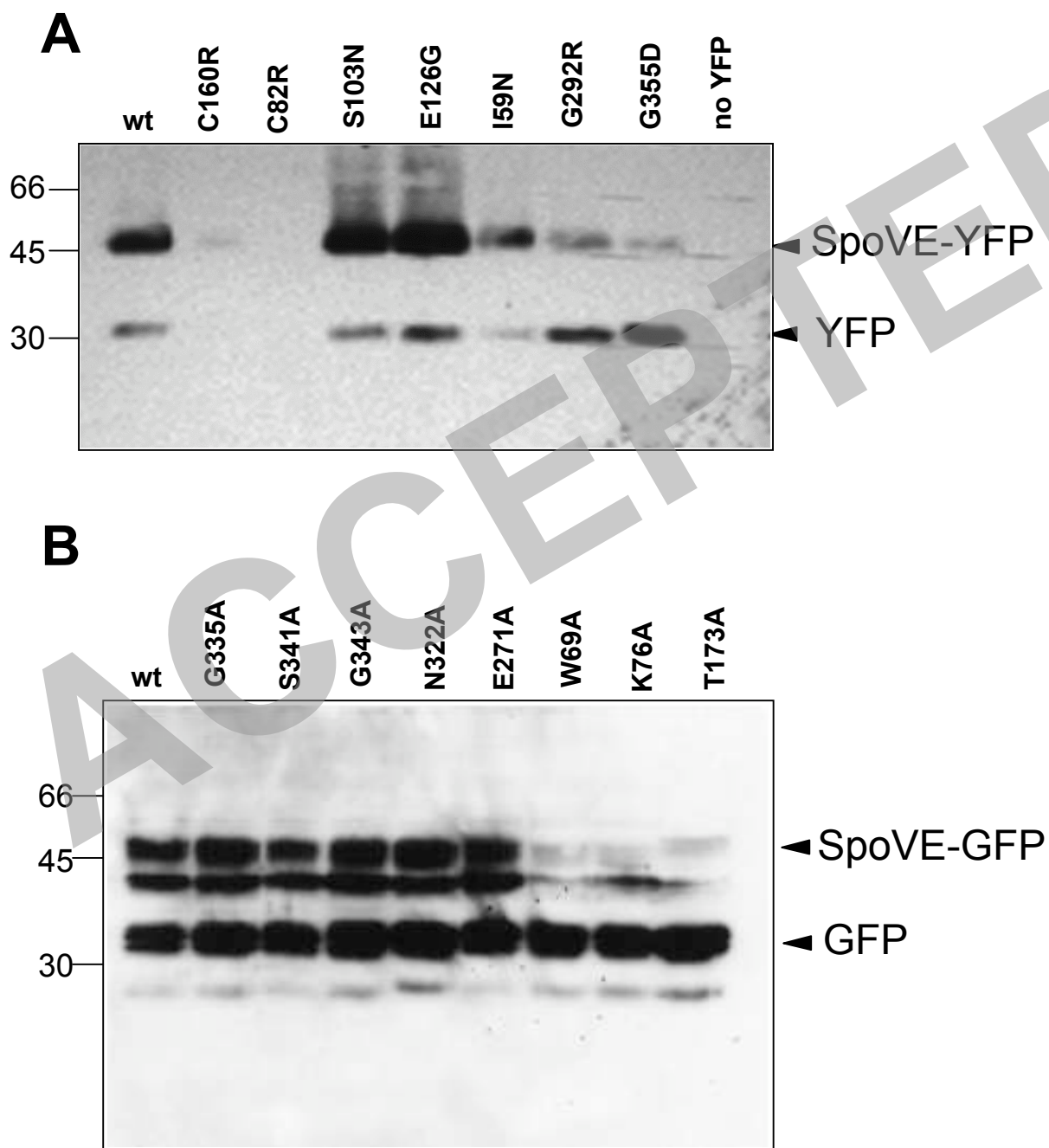
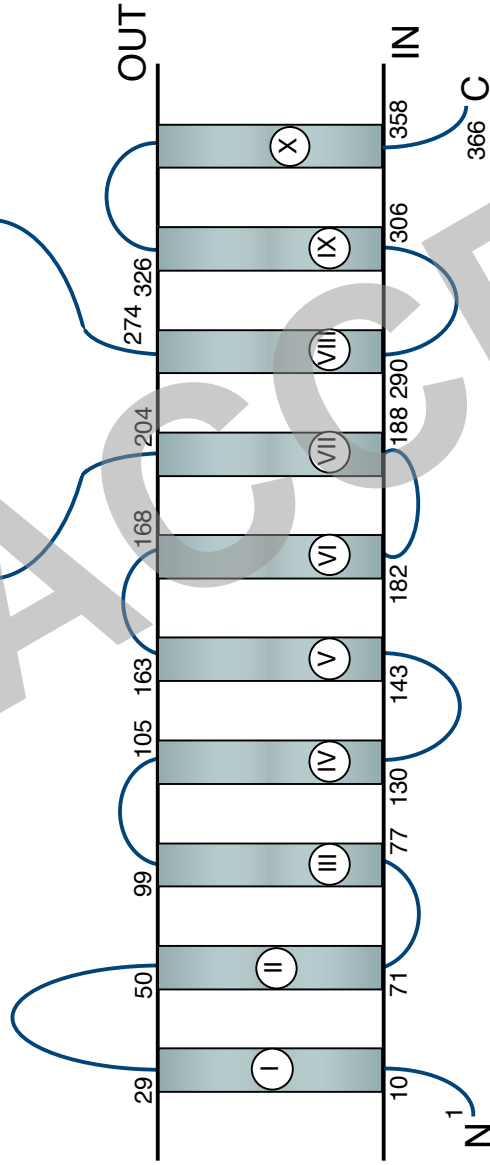


Figure 6



Supplementary Figure 1



Region	Residue Range	Sequence
TM II	58-71	GIGV I AMRF GIGV I AMRF GIGV I AMRF GVGV V AMRF GVGV V AMRF GTGV L LMRV GLGV V AMRF
	71-103	IAGGALFAL ALGTV I FAC IAGFV LFA I AIGTVMLR I GIGAVV I RA AIGTVMLR I LLGAVA I EV LLGISV I EG VIGAGLMES IIGVLLQL IIGVLLQL LIGFVLMKV IIGVLLQL
	103-116	NGSR S W IGV NGSR S W IGV NGSR S W IGV GGAR S W IGI GGAR S W IGI GGAR S W LGV GGAR S W IGI GNAQ S WFKI GNAQ S WFRV GNAQ S WFKI NGAKGW I - - NGAQRWVFG NGAKGW I - - KGAK S WFR I NGAK S W FQF NGAK S WFKI LGAKRWFV LGAKRWFV KGATRW IGI LGAKRWFV
	116-160	IQPS E FMKL IQPS E FMKL IQPS E FMKL IQPS E FMKF IQPS E FMKF IQPS E FMKM IQPS E FMKF IQPS E FMKF IQPS E FMKL IQPS E FMKL IQPS E FMKL IQPA E FVK I IQPS E FMK I IQPA E FVK I IQPS E FMKV LQPS E FMK I LQPS E FTK I LQPS E FFK I IQPS E FFK I IQPS E FFK I YQPS E VMK I IQPS E FFK I
	160-271	L I I M C Q P D L L I I M Q P D L L I I M Q P D L I I I M C Q P D L G M I M L Q P D L G M I M L Q P D L A L I M M Q P D L G M I M L Q P D L G L I A M Q P D F A L V A A Q P D V A L I A I Q P D F V L I L Q N D L F L I L K Q P D L V L I L Q N D L G L I L M Q - D A G L I L M Q - D A G M I V L Q - D A A V V Y S Q P D T A V V Y S Q P D T Y L V L K Q P D L A V V Y S Q P D T
	271-322	A I L S E E L G F A I L S E E L G F A I L S E E L G F A I L S E E L G F A I L S E E L G F A I L S E E M G F A I L S E E L G F A I L S E E L G I A V I A E E L G I A I I A E E L G I A V I S E E L G I A I I S E E L G F A V I G E E F G F A I I S E E L G F S I I G E S F G F A V I G E S F G F A I L G E S F G F A T I A E E G G F A T I A E E G G F A V I G E E F G F A I I A E E G G F
	322-358	Q V V M I N I G V V Q V V M I N I G V V Q V V M I N I G V V Q V V M I N I G V V Q V V M I N I G V V Q V V M I N I G V V Q V V M I N I G V V Q V V M I N I G V V Q V V M I N I G V V Q S F V N L G G I Q S F V N L G G I Q T F V N I G V G M Q T F V N I G V G M Q T F V N I G M N Q T F V N I G M N H T F Q N I G M N H T F Q N I G M N H T F Q N I G M I Q I F Q N I A M T Q I F Q N I A M T Q I F Q N I G M I Q I F Q N I G M I
	358-366	LMA R 55 VGV LLN LMA VGV LLN LAA VGV LLN LMA VGV LLN LMA VGV LLN LMA VGV LLN LVS VGV LLN LMA VGV LLN LMA VGV LLN LGS MGI LAN MAS AGI LYN LMS AGI LYN L I A MGI LLN MMA IGI VLN L I A MGI LLN L I G MGI VYN L I G FGI VYN L I G YAI VYN L I S FGI VYN M I M MGI ILS M I M MGI ILS MVA MGI VLN M I M MGI ILS